


RESEARCH

Open Access



# Exosomes derived from a mesenchymal-like endometrial regenerative cells ameliorate renal ischemia reperfusion injury through delivery of CD73

Bo Shao<sup>1,2†</sup>, Hong-da Wang<sup>1,2†</sup>, Shao-hua Ren<sup>1,2,4†</sup>, Qiang Chen<sup>1,2</sup>, Zhao-bo Wang<sup>1,2</sup>, Yi-ni Xu<sup>1,2</sup>, Tong Liu<sup>1,2</sup>, Cheng-lu Sun<sup>1,2</sup>, Yi-yi Xiao<sup>1,2</sup>, Hong-yu Jiang<sup>1,2</sup>, Yi-cheng Li<sup>1,2</sup>, Peng-yu Zhao<sup>1,2</sup>, Guang-mei Yang<sup>1,2</sup>, Xu Liu<sup>1,2</sup>, Yu-fan Ren<sup>1,2</sup> and Hao Wang<sup>1,2,3\*</sup> 

## Abstract

**Background** Renal ischemia reperfusion (I/R) injury is a major contributor to graft dysfunction and inflammation leading to graft loss. The deregulation of purinergic signaling has been implicated in the pathogenesis of renal I/R injury. CD73 and the generation of adenosine during purine metabolism to protect against renal I/R injury. A mesenchymal-like endometrial regenerative cell (ERC) has demonstrated a significant therapeutic effect on renal I/R injury. CD73 is a phenotypic marker of human endometrial regenerative cell exosomes (ERC-Exo). However, its immunosuppressive function in regulating purinergic metabolism has been largely neglected. Here, we investigate the protective effects and mechanism of ERC-Exo against renal I/R injury.

**Methods** Lentivirus-mediated CRISPR-Cas9 technology was employed to obtain CD73-specific knockout ERC-Exo (CD73<sup>-/-</sup>ERC-Exo). C57BL/6 mice who underwent unilateral ureteral obstruction were divided into the Untreated, ERC-Exo-treated, and CD73<sup>-/-</sup>ERC-Exo-treated groups. Renal function and pathological injury were assessed 3 days after renal reperfusion. The infiltration of CD4<sup>+</sup> T cells and macrophages was analyzed by flow cytometry and immunofluorescence staining in kidneys. CD73-mediated immunosuppressive activity of ERC-Exo was investigated by bone marrow-derived macrophages (BMDM) co-culture assay in vitro. Flow cytometry determined macrophage polarization. ELISA and Treg proliferation assays detected the function of macrophages. Furthermore, the role of the MAPK pathway in CD73-positive Exo-induced macrophage polarization was also elucidated.

**Results** Compared with Untreated and CD73<sup>-/-</sup>ERC-Exo-treated groups, CD73-positive Exo effectively improved the serum creatinine (sCr), blood urea nitrogen (BUN), and necrosis and detachment of tubular epithelial cells, necrosis and proteinaceous casts induced by ischemia. CD73 improved the capacity of ERC-Exo on CD4<sup>+</sup> T cell differentiation in the renal immune microenvironment. Surprisingly, ERC-Exosomal CD73 significantly decreased the populations of M1 cells but increased the proportions of M2 in kidneys. Furthermore, CD73-positive Exo markedly reduced the levels of proinflammatory cytokines (IL-1 $\beta$ , IL-6, and TNF- $\alpha$ ) and increased anti-inflammatory factors (IL-10) level

<sup>†</sup>Bo Shao, Hong-da Wang, and Shao-hua Ren have contributed equally to this article.

\*Correspondence:

Hao Wang

hwangca272@hotmail.com; hwang1@tmu.edu.cn

Full list of author information is available at the end of the article



© The Author(s) 2025. **Open Access** This article is licensed under a Creative Commons Attribution-NonCommercial-NoDerivatives 4.0 International License, which permits any non-commercial use, sharing, distribution and reproduction in any medium or format, as long as you give appropriate credit to the original author(s) and the source, provide a link to the Creative Commons licence, and indicate if you modified the licensed material. You do not have permission under this licence to share adapted material derived from this article or parts of it. The images or other third party material in this article are included in the article's Creative Commons licence, unless indicated otherwise in a credit line to the material. If material is not included in the article's Creative Commons licence and your intended use is not permitted by statutory regulation or exceeds the permitted use, you will need to obtain permission directly from the copyright holder. To view a copy of this licence, visit <http://creativecommons.org/licenses/by-nc-nd/4.0/>.

in kidneys. ERC-Exosomal CD73 improved macrophage immunoregulatory function associated with the MAPK pathway (including ERK1/2 and p38 pathways), which exerted a potent therapeutic effect against renal I/R.

**Conclusions** These data collected insight into how ERC-Exo facilitated the hydrolysis of proinflammatory ATP to immunosuppressive ADO via CD73. CD73 is a critical modulator of the MAPK signaling pathway, inducing a polarization shift of macrophages towards an anti-inflammatory phenotype. This study highlights the significance of ERC-Exosomal CD73 in contributing to the therapeutic effects against renal I/R.

**Keywords** Renal ischemia–reperfusion injury, CD73, Human endometrial regenerative cells, Exosome, Macrophage

## Introduction

Renal ischemia–reperfusion (I/R) injury represents the predominant cause of acute kidney injury (AKI), manifesting as an abrupt decline in renal functionality [1]. Renal I/R injury has remained a major obstacle contributing to primary graft dysfunction, delayed graft function and graft failure [2]. The deregulation of purinergic signaling has been implicated in the pathogenesis of renal I/R injury. The functional activities of ectonucleotidases such as CD73, which hydrolyse pro-inflammatory ATP to generate immunosuppressive adenosine, are therefore pivotal in acute inflammation. Alterations in the expression of ectonucleotidases on various immune cells, such as T cells and macrophages, as well as the renal tubular epithelial cells, control purinergic receptor-mediated effects on target tissues within the kidney. The novel drugs targeting purinergic processes could lead to effective therapies for the management of renal I/R injury.

Stem cells are being studied as a therapeutic tool to treat several diseases, including kidney disease [3]. Endometrial regenerative cells (ERC), a type of mesenchymal stromal cells (MSC) isolated from menstrual blood, have been shown to retain fundamental MSC properties [4]. Easy to obtain, ethically unobjectionable, and short doubling time make ERC a promising candidate for MSC-based therapy [5]. Nevertheless, allogeneic MSC remain constrained by several factors in their clinical implementation, including the potential for immune rejection, the risk of tumor formation, and other considerations [6, 7]. Exosomes, defined as extracellular vesicles with a diameter of 30–150 nm, hold significant promise for the clinical treatment of a wide range of diseases [8]. Several studies have indicated that exosomes promoted tissue repair, attenuated cell apoptosis and immunomodulatory potential via transferring functional miRNAs or proteins [9–11]. Our previous study also confirmed that exosomes derived from ERC (ERC-Exo) had a therapeutic effect similar to ERC, which could effectively and safely remodel the mucosal pathological damage in experimental colitis mice [12]. The potential mechanisms of the protection provided by ERC-Exo in renal I/R have not been elucidated. Based on the above findings, we speculate that

ERC-Exo may restore the renal function of renal I/R mice by transferring ERC-Exo-containing proteins.

This study found that CD73 protein levels were significantly high in ERC-derived exosome. Specifically, ERC-Exo can alleviate renal I/R by delivering CD73 in the injured kidney. Under the stimulation of pathological factors, aberrant purinergic metabolism, especially the massive release of inflammatory mediator ATP into the extracellular matrix, is activated as a key initiating factor that promotes kidney injury. We assessed whether ERC exosomal CD73 can hydrolyze ATP effectively to mediate M2-like macrophage polarization through a MAPK-dependent pathway, protect renal tubular epithelial cells, and promote renal injury repair.

## Materials and methods

### Culture and characterization of ERC

After filling out the informed consent letter, all human menstrual blood samples were obtained from Tianjin Medical University General Hospital from healthy female volunteers (20–30 years of age). ERC derived from the menstrual blood of adults was isolated and cultured as previously described [13]. In brief, mononuclear cells were isolated from the menstrual blood by Ficoll density centrifugation using a sterile menstrual cup. The isolated cells were subsequently cultured in Dulbecco's Modified Eagle Medium/Nutrient Mixture F12 (DMEM/F12, Hyclone, USA) containing 10% Fetal Bovine Serum (FBS, Hyclone, USA) and 1% penicillin/streptomycin (Solarbio, Beijing, China) at 37 °C, 5% CO<sub>2</sub>, and normoxia. The culture medium was changed every 3 days to remove tissue fragments and non-adherent cells. The adherent cells were passaged utilizing a 0.25% Trypsin solution (with EDTA; Solarbio, Beijing, China). Generation 3 cells were used for subsequent ERC characterization.

Various methodologies are available for the minimal criteria of MSC including surface molecules and differentiation assays by the International Society for Cell & Gene Therapy (ISCT) guidelines [14]. Photographed and recorded ERC of different generations. Purified passage 3 ERC were obtained and stained with fluorescent antibodies to surface molecules (CD44, CD73, CD90, CD45, CD79a, and HLA-DR) (eBioscience, California, USA).

Additionally, their osteoblastic, adipocytic, or chondrocytic differentiation potential under defined conditions was demonstrated by in vitro staining according to the manufacturer's protocol (TransGen Biotech, Beijing, China).

#### Preparation of ERC with CD73 knockout

To knockout CD73 (*NT5E*, NM\_002526) in ERC, lentivirus-mediated CRISPR-Cas9 knockout technology was applied by the manufacturer's instructions (GeneChem Inc., Shanghai, China). The vector was U6-sgRNA-EF1a-Cas9-FLAG-P2A-Puromycin. Synthetic single guide RNA (sgRNA) targeting human *NT5E* sequences were designed with two targeting sequences: 5'-CACTTTCTGAGCGATGAGTT-3' and 5'-CACCGAACTCATCGCTCAGAAAGT-3'. The lentiviral infection protocol was conducted in a biosafety cabinet with an optimized multiplicity of infection (MOI=30). The transfected cells were passaged when they reached 80% confluence. Following puromycin selection (2 µg/mL, Solarbio, Beijing, China), the efficiency of *NT5E* knockout was examined by Western blotting and flow cytometry, and subsequent experiments were performed from passages 5–7.

#### Isolation, purification, and characterization of exosomes

As previously described, exosomes were collected from cell culture supernatants by ultracentrifuge [15]. In brief, ERC were maintained in exosome depleted human MSCs medium (MM101, TransGen Biotech, China) for 48 h to harvest conditioned medium. The conditioned medium was centrifuged at 2,000 g for 20 min at 4 °C to remove apoptotic cells and cell debris and then at 10,000 g for 30 min to remove comparatively larger microvesicles. The clarified supernatants were filtered through 0.22 µm filter membranes. Finally, the supernatant was ultracentrifuged at 130,000 g (Optima XPN-100, Beckman Coulter, USA) for 2 h at 4 °C to obtain exosomes, then washed with PBS and ultracentrifuged at 130,000 g for another 2 h. The concentration was determined using a BCA protein assay kit. (PC0020, Solarbio, China). The morphology of ERC-exo was observed by transmission electron microscopy (TEM) (H7800, HitachiLtd., Japan). Particle size was determined by nanoparticle tracking analysis (NTA; ZetaViewPMX 110). Surface markers, including exosomal markers (CD63, CD9, TSG101) and Golgi markers (Calnexin), were analyzed by Western blotting.

#### Co-cultures of exosomes with splenocytes

To isolate splenocytes, spleen mechanically mashed and subjected to erythrocyte lysis as previously described [16]. Splenocytes ( $1 \times 10^6$  cells/well) were seeded in 96 well plates and were randomly assigned to 4 groups: LPS group, LPS+Exo group, LPS+NC-Exo group (ERC

transfected with lentiviral lacking *NT5E* gene, used as negative control), and LPS+CD73<sup>-/-</sup> Exo group (ERC transfected with lentiviral to delete *NT5E* gene). The cell proliferation ability was analyzed by the CCK-8 kit (n=5 in each group). Additionally, splenocytes stimulated with various stimulators (St) were co-cultured with exosomes for 72 h. Macrophages were stimulated with LPS (2 µg/mL), and T cells were stimulated with 5 µg/mL precoated anti-mouse CD3 (Biolegend, USA) and 3 µg/mL anti-mouse CD28 (BioLegend, USA). The percentages of each cell type were examined by FACS analysis.

#### HK2 cell culture and H/R model

HK2 cells purchased from ATCC were cultured in DMEM/F12 supplemented with 10% FBS, 1% penicillin/streptomycin (Solarbio, Beijing, China) at 37 °C in a humidified atmosphere containing 5% CO<sub>2</sub>. For hypoxia/reoxygenation (H/R) treatment, HK2 cells were exposed to hypoxia condition with 1% O<sub>2</sub>, 5% CO<sub>2</sub>, and 94% N<sub>2</sub> for 24 h followed by reoxygenation (21% O<sub>2</sub>, 5% CO<sub>2</sub>, and 74% N<sub>2</sub>) for 12 h. HK2 cells were randomly assigned to 3 groups: H/R, H/R+Exo, H/R+CD73<sup>-/-</sup> Exo, (n=5 in each group). Next, the cells were incubated with the CCK-8 Kit (10 µL/well; #96992, Sigma) for 2 h. Finally, the absorbance was recorded at 450 nm utilizing a microplate reader (Safire2, TECAN, Switzerland).

#### Measurement of the AMP hydrolytic of exosomes

The AMPase enzymatic activity of exosomes was assessed with the assistance of the Phosphate Assay Kit (ab270004, Abcam, USA). To remove inorganic phosphate in PBS, exosomes were isolated by ultracentrifugation and then resuspended in MES buffer (M1317, Sigma, USA). 100 µM AMP (HY-A0181, MedChemExpress, China) was added to 500 µl MES buffer, followed by the addition of 30 µg/ml ERC-Exo or CD73<sup>-/-</sup> ERC-Exo, and incubation at 37 °C for 1 h. The Adenosine Assay Kit (Bio-Vision, CA, USA) and the Phosphate Assay Kit (ab270004, Abcam) were employed for measuring the enzymatic activity of ERC-Exo.

#### Exosome labeling and bioluminescence in vivo

To obtain DiO-labelled or PKH26-labelled exosomes, donor ERC or CD73<sup>-/-</sup>ERC were labeled with DiO (C1038, Beyotime, China) or PKH26 (MINI26, Sigma-Aldrich, USA), respectively, according to the manufacturer's protocol. Subsequently, the cells were washed twice with exosome-depleted human MSCs medium to remove excess dye. After 48 h, the supernatants were harvested, and exosomes were isolated, as described above. This allows us to remove most of the free dye in the pellet. To assess the in vivo tissue distribution of ERC-Exo, control mice or renal I/R injury mice were injected intravenously

with 200 µg of DIO-labelled ERC-Exo. Mice were euthanized 12 h after injection. Tissues, including lung, heart, liver, spleen, and kidney, were resected and imaged using the IVIS Spectrum imaging system (Xenogen, Inc.).

#### Ethics approval and consent to participate

This study was performed following the Declaration of Helsinki Ethical Principles and approved by the Ethics Committee of the Tianjin Medical University General Hospital, Tianjin, China (Approval number: IRB2024-YX-014-01): (1) Title of the approved project: Studies on the mechanism of human menstrual blood-derived endometrial regenerative cell exosomes in the therapy of ischaemia–reperfusion. (2) Name of the institutional approval committee: the Ethics Committee of the Tianjin Medical University General Hospital, Tianjin, China. (3) Approval number: IRB2024-YX-014-01. (4) Date of approval: 01/25/2024.

#### Animal study

The 45 male C57BL/6 mice, aged 8–10 weeks, were acquired from Tianjin Medical University General Hospital. The animal care and experimental protocols were approved by the Institutional Animal Care and Use Committee of Tianjin Medical University General Hospital and was conducted in accordance with the ARRIVE guidelines 2.0 (Project title: Studies on the mechanism of human menstrual blood-derived endometrial regenerative cell exosomes in the therapy of ischaemia–reperfusion; Approval number: IRB2024-DW-08; Date of approval: 01/30/2024). For two weeks, all mice were maintained in a controlled environment with unrestricted access to food and water.

#### Animal models and therapeutic experiments

The work has been reported in line with the ARRIVE guidelines 2.0. By IACUC guidelines, mice were observed daily after surgery, and euthanasia was indicated for mice using a scoring system to evaluate excessive distress, including the presence of excessive weight loss, loss of thermoregulation, and lethargy. The mice were randomly assigned to the following groups. All the animals were ear tagged and randomly grouped by computer. Start with any number in the random number table and obtain N random numbers sequentially in the same direction. The remainder is obtained by dividing the random number by the number of groups, and if it is divided, the remainder is obtained by the number of groups. Finally, group by remainder. Male C57BL/6 mice (8–10 weeks old) were anesthetized with 1% pentobarbital before undergoing surgery and then placed on a heated pad to help maintain body temperature. Renal I/R injury was established as previously reported[17]. Specifically, the

two renal pedicles were clamped with microaneurysm clamps for 40 min. The clamps were then released, and the kidneys were observed by a color change to confirm blood reflux before the incision was closed. Sham operations were performed in which both kidneys were exposed, but no renal pedicle clamping was performed. Body temperature was maintained at 36.6–37.2 °C on a heating pad throughout the procedure using a sensitive rectal probe. Generally, mice were divided into three groups: Untreated, ERC-Exo, CD73<sup>-/-</sup> ERC-Exo, with 6 mice per group. ERC-Exo or CD73<sup>-/-</sup> ERC-Exo (200 µg) were administered intravenously after reperfusion, thrice every 24 h. At 72 h after reperfusion, The mice were euthanized by cervical dislocation after sampling. Kidneys were rapidly harvested for histological assessment, molecular biology testing, and flow cytometry analysis of inflammatory cells. For histopathology, sections of the kidney were fixed in 10% buffered formalin. All the above operations were performed at the Animal Center of Tianjin Medical University General Hospital. The experimenter does not participate in the assignment process, but only knows the final assignment result. Results evaluation and data analysis were performed by a third party, and at least two researchers were asked to cross-check the analysis results.

#### Renal function and histological assessment

Serum sCr and BUN concentrations were measured using commercially available assay kits (Nanjing Jiancheng, Nanjing, China). For histological evaluation, the kidney tissue was perfused with PBS, fixed in 10% buffered formalin, embedded in paraffin, sectioned at a thickness of 5 µm, and stained with the periodic acid Schiff (PAS) staining kit (G1281, Solarbio, China). The tubular injury score based on a semi-quantitative assessment of tubular rupture, dilatation, rupture, and casts was assessed on ten random tissue sections per mouse [18]. The scoring range was 0–5: 0, no lesion; 1, < 10%; 2, 10 to 25%; 3, 26 to 50%; 4, 51 to 75%; 5, > 75%.

#### Laser doppler perfusion imaging

To measure the renal blood flow, we are going to perform the Laser Doppler perfusion imager by a LDI system (PeriCam PSI System) before ischemia insult (0), after 40 min of ischemia (40 min) and after 72 h of reperfusion (72h). Simultaneously, images were analysed using Pericam PSI software, and the perfusion value was calculated and divided by the baseline measurement to obtain a percentage representing the relative changes in blood flow.

#### TUNEL staining

The 3 µm section of kidney tissue was deparaffinized. Apoptotic cells were then demonstrated with the



commercial TdT-mediated dUTP nick end labeling (TUNEL) kit (K1133, Apexbio, USA). Green TUNEL-positive nuclei were observed and photographed using a fluorescence microscope. TUNEL-positive cells were counted in 6 fields (400×) per slide using a fluorescence microscope (Olympus, Japan) according to the manufacturer's protocol.

### Flow cytometry

For the detection of immune cell phenotypes in kidneys, mononuclear cells from kidneys were isolated according to the previously described method [19]. Both kidneys were minced and incubated in collagenase D (5 mg/mL, Sigma-Aldrich) solution for 30 min at 37 °C. Single cell suspensions of kidney digestions were obtained by mechanical disruption of tissues using 70-µm strainers (BD Bioscience), and kidney mononuclear cells were isolated using isotonic Percoll density gradient centrifugation. As previously described, flow cytometric analysis was performed [20]. Specifically, cells were stained in FACS buffer (PBS, 2% FBS, 0.1% sodium azide) and pre-incubated with anti-CD16/CD32 antibody for 15 min to reduce non-specific binding through the Fc receptor. Fluorochrome conjugated monoclonal antibodies (mAbs) including CD45-APC, CD4-FITC, CD11b-FITC, F4/80-APC, CD86-PerCP-Cyanine5.5, IFN-γ-PE, IL-17-PerCP-Cyanine5.5, and CD206-PE were purchased from BioLegend, Inc.. In addition, cells from the kidneys were fixed and permeabilized using a Cytofix/Cytoperm™ Fixation/Permeabilization Kit (BD, USA) and stained intracellularly for IFN-γ-PE, IL-17-PerCP-Cyanine5.5, Foxp3-APC, and CD206-PE. They were incubated with the appropriate cocktail of fluorochrome-conjugated monoclonal antibodies for 50 min at 4 °C, washed, and resuspended in FACS buffer. Samples were analyzed on a BD FACS Canto™ II flow cytometer and FlowJo 10.8.1.

### Immunofluorescence

Renal inflammatory macrophage infiltration was assessed by immunofluorescence. The kidneys were removed, fixed in 10% buffered formalin, embedded in paraffin, and cut into 3 µm-thick sections. Then, the sections were permeabilized with Triton X-100 (0.2%) in PBS, followed by blocking with 10% goat serum. Sections were stained with the following antibodies: rat anti-mouse F4/80 antibody (1:200, ab6640, Abcam) and rabbit anti-mouse iNOS antibody (1:250, ab178945, Abcam), rabbit anti-mouse CD206 antibody (1: 500, ab64693, Abcam). Fluorescence-conjugated secondary antibodies were mixed and used as the second antibodies. Positive cells in the cortex were numbered in five non-overlapping fields of view at 400× magnification and the average cell counts were used for analysis.

### Bone marrow derived macrophages (BMDMs)

To isolate BMDMs, bone marrow cavities were rinsed with PBS, which were then filtered and subjected to erythrocyte lysis as previously described [21]. Isolated cells were grown in high glucose DMEM (Gibco, USA) supplemented with 10% FBS, 1% penicillin/streptomycin, and 20 ng/mL recombinant mouse macrophage colony-stimulating factor (M-CSF) (RP01206, Abclonal, China), with the medium being changed every 2 to 3 days. Mature BMDMs were randomly assigned to 4 groups: LPS, LPS+Exo, LPS+CD73<sup>-/-</sup> Exo, and LPS+CD73<sup>-/-</sup>Exo+Recombinant CD73 Protein (30 ng/mL, RP01447, Abclonal) (n=3 in each group). BMDMs isolated from the different treatment groups were analyzed for phenotype, protein expression, and cytokine secretion.

### Cellular uptake of exosome in vitro

PKH26-labelled ERC-Exo or CD73<sup>-/-</sup> ERC-Exo were incubated with BMDMs for 3 h. After three washes with PBS, BMDMs incubated with ERC-Exo or CD73<sup>-/-</sup> ERC-Exo were fixed with 4% PFA, blocked for 20 min at room temperature, and incubated with anti-F4/80 antibody (1:200, ab6640, Abcam) at 4 °C overnight. After three washes with PBS, the cells were incubated with FITC-conjugated anti-rat secondary antibody (1:500, ab150157, Abcam) for 1.5 h at room temperature. The cells were washed 3 times with PBS, and the nuclei were counterstained with DAPI (ab285390, Abcam, USA). Fluorescence imaging was performed by a fluorescence microscope (Olympus, Japan) and analyzed using the Image J software.

### Western blotting

ERC-exo, BMDMs, and kidney tissues were lysed in RIPA lysis buffer (R0010, Solarbio, China) containing protease (K1007, APExBIO, USA) and phosphatase inhibitor cocktail (K4003, APExBIO, USA). The BCA assay (PC0020, Solarbio, China) determined protein concentration according to the manufacturer's instructions. Equal protein samples (40 µg per lane) were separated by 10% SDS-PAGE. The samples were transferred to PVDF membranes (0.45 µm; Millipore). The membranes were blocked in TBST with 5% BSA for 2 h at room temperature and incubated with primary antibodies as follows: CD63 (1:1000, A19023, ABclonal), CD81 (1:1000, A4863, ABclonal), TSG101 (1:1000, A5789, ABclonal), Calnexin (1:1000, A4846, ABclonal), Arginase-1 (1:1000, 93668S, CST), iNOS (1:1000, 13120S, CST), ERK1/2 (1:1000, A4782, ABclonal), P-ERK1/2 (1:1000, AP0485, ABclonal), P38 (1:1000, A4771, CST), P-P38 (1:1000, AP1311, ABclonal), and GAPDH (1:1000, 2118S, CST) at 4 °C overnight. The membranes were washed three times in

TBST (15 min each time) and then incubated with HRP-conjugated secondary antibody (1:3000, #7074S; CST) for 40 min at room temperature. The membranes were detected by enhanced chemiluminescence (WP20005, Thermo Fisher Scientific, USA) after three washes (15 min each). The densitometry of protein bands was quantified and analyzed using ImageJ software.

#### Co-culture of macrophages and T cells

CD4<sup>+</sup> naïve T cells were isolated from splenocytes using CD4 (L3-T4) Microbeads (130-117-043, Miltenyi Biotec) and seeded into 96-well plates (10<sup>5</sup>/well) supplemented with 10 ng/mL recombinant IL-2 (Abclonal, China), 5 µg/mL precoated anti-mouse CD3 (Biolegend, USA) and 3 µg/mL anti-mouse CD28 (BioLegend, USA). BMDMs were seeded in 96-well plates and allowed to acclimate for 24 h. Macrophages were primed with 200 ng/mL LPS for 48 h and washed 3 times. CD4<sup>+</sup> T cells in a complete medium were added to the macrophage and co-cultured for another 72 h. These cells were maintained in a CO<sub>2</sub> (5%) incubator at 37 °C. Staining was carried out using a Cytotfix/Cytoperm™ Fixation/Permeabilization Kit (BD, USA) according to the manufacturer's instructions. Tregs were stained using a fluorescent-conjugated anti-Foxp3-APC (1:100, BioLegend, USA). Samples were analyzed on a BDFACS Canto™ II flow cytometer and FlowJo 10.8.1.

#### Enzyme-linked immunosorbent assay (ELISA)

The concentrations of IL-6, IL-1 β, TNF-α, and IL-10 in kidney homogenate and cell supernatants were assessed using corresponding commercial ELISA kits (DAKEWE, China) following the manufacturer's instructions. The optical density (OD) value was measured with a microplate reader (Safire2, TECAN, Switzerland).

#### Statistical analysis

Graphing and statistical analyses were performed using GraphPad Prism v.9.5.0 (GraphPad Software). Results are expressed as mean ± standard error of the mean (SEM). The Shapiro–Wilk test was used to assess the normality of continuous variables. Unpaired two-tailed Student's t-tests between two groups and one-way ANOVA followed by Tukey's multiple comparison post hoc test were used to test differences among multiple groups. Statistical significance was set at \**P* < 0.05, \*\**P* < 0.01, \*\*\**P* < 0.001, and the most significant for \*\*\*\**P* < 0.0001.

## Results

### Characterization of ERC

Microscopic examination showed the spindle-shaped morphology of ERC adhering to the walls of the culture flasks (Fig. 1A). Furthermore, the flow cytometry

identification of surface markers on MSC-like ERC were positive for phenotypic markers of CD44, CD73, and CD90 but were negative for CD45, CD79α, and HLA-DR (Fig. 1B). In addition, ERC demonstrated the potential to differentiate into adipocytes, chondrocytes, and osteocytes under specific differentiation conditions (Fig. 1C). Therefore, these population cells from endometrial blood meet the minimal criteria given to MSCs by the International Society for Cell & Gene Therapy (ISCT) guidelines.

### Construction and identification of CD73<sup>-/-</sup>ERC-derived exosome

To obtain CD73<sup>-/-</sup>ERC-Exo, the *NT5E* gene (code CD73) in ERC was deleted using lentivirus-mediated CRISPR-Cas9 technology. Immune cell co-culture studies showed that altering CD73 did not alter many other genes (Additional file 3: Fig. S1). As illustrated in Fig. 2A, the successful knockout of CD73 (CD73<sup>-/-</sup>ERC) was validated by flow cytometry. TEM and NTA were then used to analyze the size and morphology of exosomes purified from ERC and CD73<sup>-/-</sup>ERC conditioned medium. TEM images showed that ERC-Exo and CD73<sup>-/-</sup>ERC-Exo exhibited homogeneous size, circular shape, and double-layered membrane vesicle structures by the typical characteristics of exosome (Fig. 2B). NTA revealed that the mean diameters of ERC-Exo and CD73<sup>-/-</sup>ERC-Exo were 130 nm and 135 nm respectively, consistent with the definition of exosome (Fig. 2C). Both ERC-Exo and CD73<sup>-/-</sup>ERC-Exo were found to be enriched with CD9, CD81, and TSG101 (exosome positive markers), but not Calnexin (an exosome negative marker) (Fig. 2D), suggesting that the CD73 knockout did not impact exosome release in ERC. These results demonstrated that the vesicles purified from the ERC exhibited characteristics consistent with the exosome, and we successfully engineered an exosome knockout of CD73.

To further verify the successful knockout of CD73 on ERC-Exo, western blot analysis in Fig. 2E, F, showed the level of CD73 was significantly reduced in CD73<sup>-/-</sup>ERC-Exo compared to ERC-Exo (*P* < 0.0001). The AMPase activity of CD73 showed that ERC-Exo hydrolyze AMP (Fig. 2G, H). However, hydrolytic effects of ERC-Exo were significantly stronger than that of CD73<sup>-/-</sup>ERC-Exo. The molecular weight was consistent with the qualities of the full-length CD73 protein (70kD), and in vitro experiments have revealed that CD73 had hydrolase activity on exosome. Therefore, CD73 anchored in ERC-Exo is protein full-length. This result further confirmed the successful knockout of

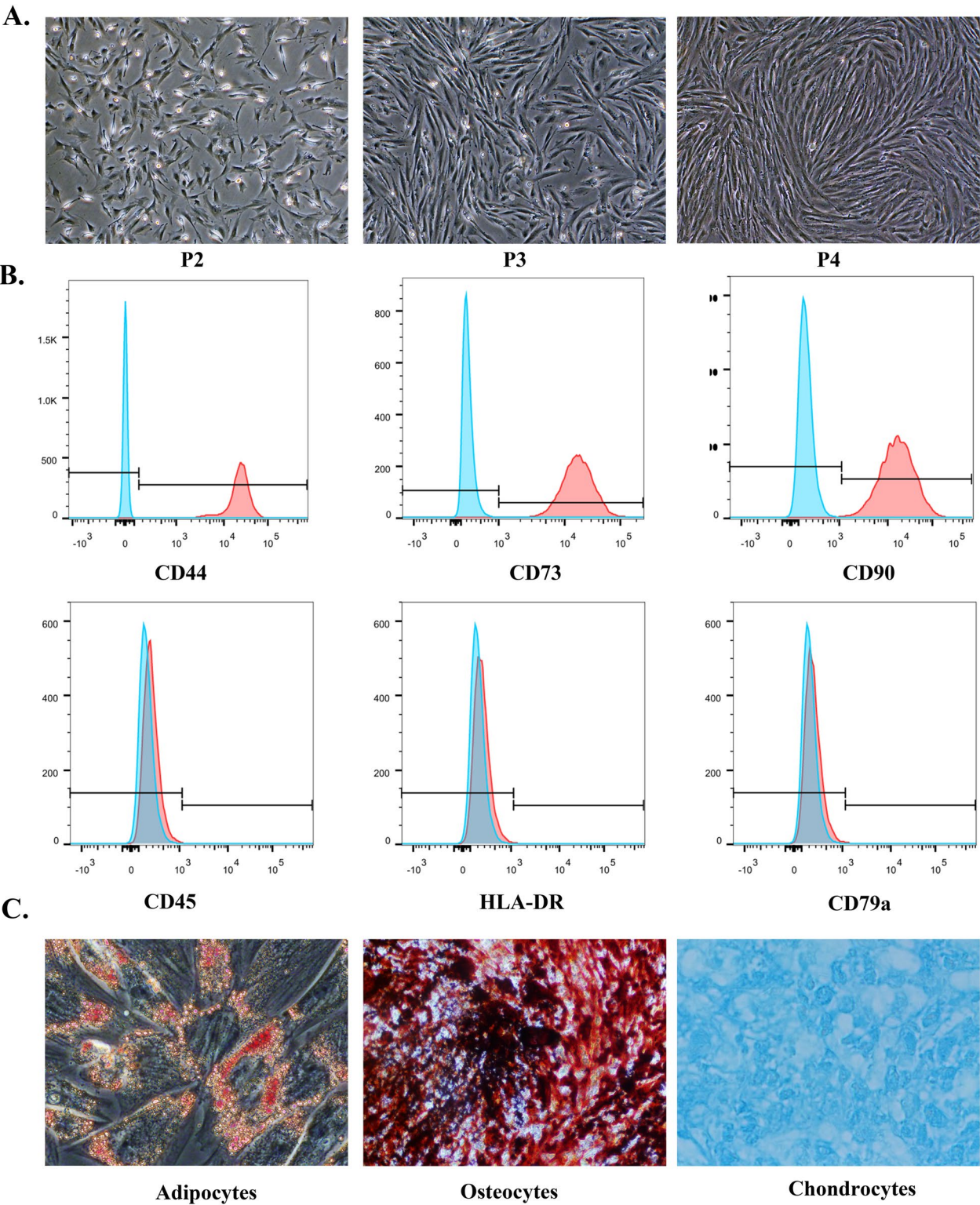


**Fig. 1** Acquisition and identification of ERC. **A** Morphology of ERC at passage 3–5 (scale bar: 250  $\mu$ m). **B** ERC were detected by flow cytometry to detect negative markers (CD45, CD79a, and HLA-DR) and positive markers (CD44, CD73, and CD90) on cell surfaces for identification. **C** The osteoblastic (Alizarin red), adipocytic (Oil red O), and chondrocytic (Alcian blue) differentiation potential of ERC



CD73 in CD73<sup>-/-</sup>ERC-Exo and the AMPase activity of CD73.

#### ERC-Exo carried CD73 to alleviate renal dysfunction and pathologic injury in renal I/R mice

Prior to evaluating the efficacy of ERC-Exo, the in vivo biodistribution of ERC-Exo was investigated with IVIS in vivo imaging analysis. ERC-Exo was investigated by labeling exosomes with DiO. We injected DiO-labelled ERC-Exo intravenously into sham or renal I/R injured mice. Ex vivo imaging of the dissected organs showed that DiO fluorescence was mainly distributed in the liver of sham mice (Fig. 3A). As shown in Fig. 3A, renal radiance signals were significantly higher in mice with I/R-induced AKI compared to Control mice. The results demonstrated that ERC-Exo had a preferential tropism for the injured kidneys.

To investigate the therapeutic efficacy of CD73 carrying ERC-Exo, a mouse model of renal I/R injury was established and ERC-Exo or CD73<sup>-/-</sup>ERC-Exo were administered intravenously after reperfusion and continued every 24 h for 3 days (Fig. 3A). Compared with the untreated group, the levels of serum creatinine (sCr) (Fig. 3F), blood urea nitrogen (BUN) (Fig. 3G), necrosis and detachment of tubular epithelial cells (TECs), necrosis and proteinaceous casts were significantly attenuated in ERC-Exo-treated mice with almost normal renal structure (Fig. 3B, D). However, ERC-Exo with CD73 knockout showed a weaker effect in ameliorating the pathological changes in mice with renal I/R injury. To assess the contributions of CD73-expressing ERC-Exo fully, kidney sections were processed for TUNEL assays to evaluate the apoptotic index for detecting injured tubules. Renal apoptosis cells in the ERC-Exo group were significantly lower than in the untreated group by severe I/R injury (Fig. 3C, E,  $P < 0.0001$ ). In contrast, knocking out CD73 reduced the efficacy of ERC-Exo in ameliorating apoptotic cells ( $P < 0.001$ ). To verify the role of CD73 carried by ERC-Exo in renal tubular epithelial cell protection, HK-2 cells exposed to hypoxia/reoxygenation (H/R) were treated with or without ERC-Exo. H/R significantly decreased cell viability rate in HK-2 cells, and these effects were partially reversed by ERC-Exo, while

Exo isolated from ERC transfected with CD73 lentivirus reduced the increase in cell viability and decrease in apoptosis caused by ERC-Exo (Fig. 3H). Together, these results demonstrated that CD73 contributed to the therapeutic efficacy of ERC-Exo against renal I/R injury.

#### Effects of CD73 carried by ERC-Exo on renal blood flow

Renal I/R injury can have dramatic effects on blood flow. Therefore, we evaluated the change in blood flow in the I/R kidneys using laser-Doppler analysis. In light of our observation of CD73 carried by ERC-Exo's protective role against renal I/R injury, we hypothesised that CD73 carried by ERC-Exo could affect renal blood flow. Laser Doppler images (Fig. 4A, B) demonstrated that impaired renal blood flow after I/R injury was restored after ERC-Exo treatment, while Exo isolated from ERC transfected with CD73 lentivirus reduced the increase in the perfusion rate caused by ERC-Exo (ERC-Exo group vs. ERC-CD73<sup>-/-</sup>Exo group,  $P < 0.01$ ).

#### CD73 improved the capacity of ERC-Exo on CD4<sup>+</sup> T cell differentiation in the renal immune microenvironment

As a key contributor to renal inflammation, T cell-mediated immune dysregulation plays an important role in the pathophysiology and pathogenesis of renal I/R injury [22]. ADO inhibited the activation of conventional CD4<sup>+</sup>T cells, which raises the question of whether CD73, the enzymatic activity of AMP to ADO, is involved in the ERC-Exo-mediated immunoregulatory responses in renal I/R injury. To further investigate this point, mononuclear cells were isolated from the kidney and detected by flow cytometry. The percentage of Th1(CD4<sup>+</sup>IFN- $\gamma$ <sup>+</sup>) and Th17(CD4<sup>+</sup>IL-17A<sup>+</sup>) cells were decreased after ERC-Exo treatment (Th1,  $P < 0.0001$ ; Th17,  $P < 0.01$ ), but this decrease was reversed by CD73<sup>-/-</sup>ERC-Exo treatment (Th1,  $P < 0.0001$ ; Th17,  $P < 0.001$ ), further suggesting that CD73 is associated with the regulation of Th1 and Th17 cells in the renal immune microenvironment (Fig. 5A–D). Additionally, we also determined the regulatory CD4<sup>+</sup>T cells, as shown in Fig. 5E, F; the ERC-Exo treated group showed a high proportion of CD4<sup>+</sup>Foxp3<sup>+</sup>Tregs, while the knockout of CD73

(See figure on next page.)

**Fig. 2** CD73 was knocked in the ERC derived exosome. **A** Flow cytometry reflected CD73 expression on the membrane of ERC and CD73<sup>-/-</sup>ERC. **B** Electron microscopy images of exosome from ERC-Exo and CD73<sup>-/-</sup>ERC-Exo (Scale bar: 200 nm). **C** Nanoparticle tracking analysis (NTA) of exosome from ERC-Exo and CD73<sup>-/-</sup>ERC-Exo. **D** Protein biomarkers of ERC-Exo and CD73<sup>-/-</sup>ERC-Exo (CD9, CD63, CD81, and Calnexin) were performed. Full-length blots/gels are presented in Additional file 1: Fig. S1. **E** Expression of CD73 in ERC-Exo and CD73<sup>-/-</sup>ERC-Exo via Western blotting. Full-length blots/gels are presented in Additional file 1: Fig. S2. **F** Gray value analysis with immunoblot based; CD73 intensity analysis was homogenized after comparing to CD9 ( $n = 3$ ). **G, H** Levels of inorganic phosphate (Pi) and Adenosine were measured after adding CD73 substrate ( $n = 3$ ). Statistical analysis was done by using unpaired two-tailed Student's t-tests. Data are presented as mean  $\pm$  s.e.m (SEM).

\*\*\*\* $P < 0.0001$ , analyzed by unpaired t-test. ERC, endometrial regenerative cell; CD73<sup>-/-</sup>ERC, ERC transfected with lentivirus; Exo, exosome



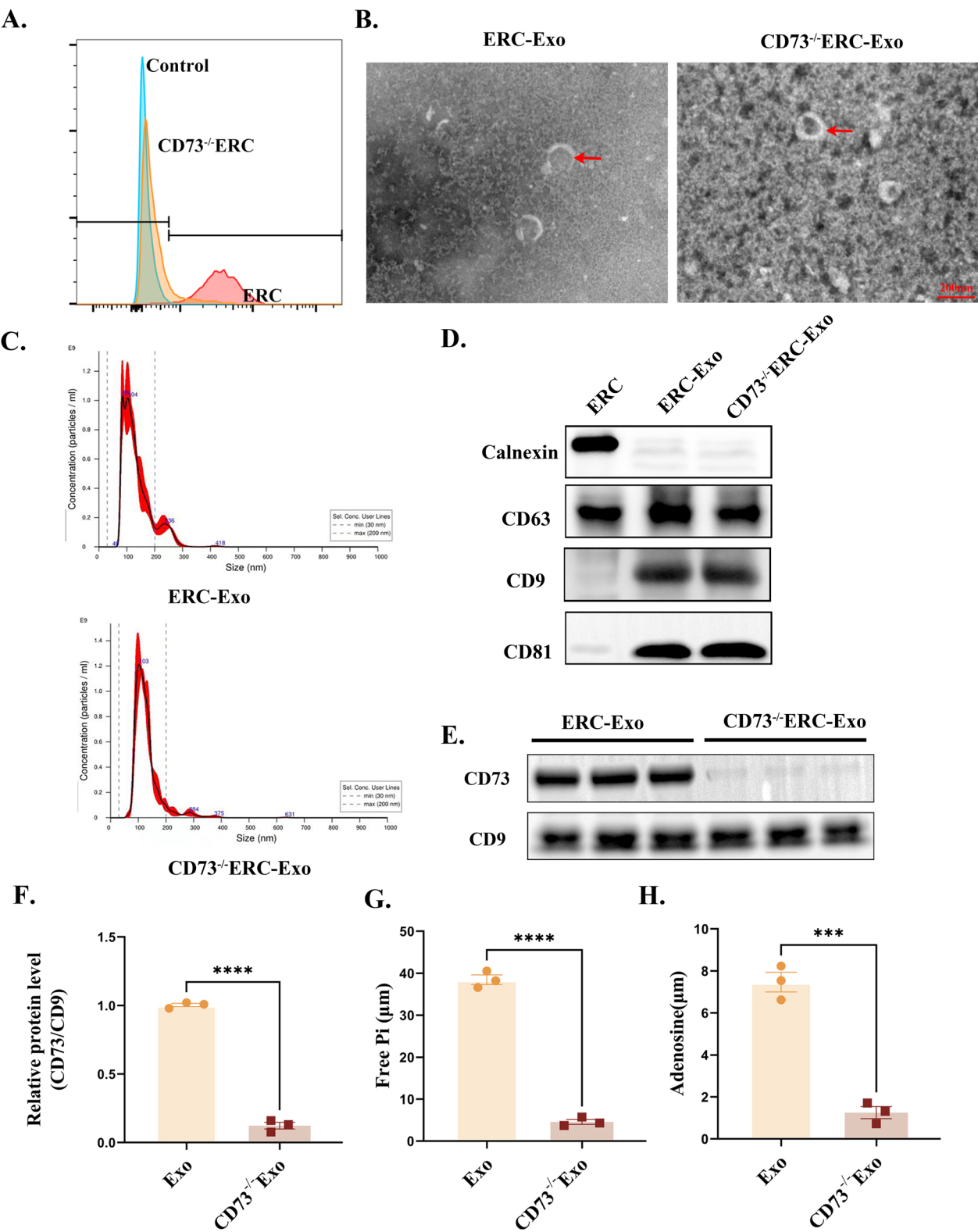


**Fig. 2** (See legend on previous page.)

attenuated the induction of Tregs. The release of cytokines is a central mediator of renal I/R injury. To further support these hypotheses, ELISA assays for pro- and anti-inflammatory cytokine profiles were conducted to examine changes in the inflammatory process. Apparently, ERC-Exo decreased the renal concentrations of IL-6, IL-1 $\beta$  and TNF- $\alpha$ , while increasing the levels of IL-10 (Fig. 5G–J, ERC-Exo-treated group *vs.* untreated group: IL-6,  $P < 0.0001$ ; IL-1 $\beta$ ,  $P < 0.0001$ ; TNF- $\alpha$ ,  $P < 0.0001$ ; IL-10,  $P < 0.0001$ ). Taken together, these data suggested that CD73 expression on ERC-Exo contributed to regulating the local CD4 $^{+}$  T cell response and cytokine profiles in renal I/R injury.

#### CD73 $^{-/-}$ ERC-exo failed to increase M2 macrophage infiltration with a concomitant decrease in M1 macrophage

Given that macrophages are dominant myeloid cell types that are critical for renal inflammation and repair following AKI, we hypothesized that ERC-Exo could alleviate renal I/R injury by modulating the phenotype of renal macrophages. Figure 6A, B demonstrated that the proportion of F4/80 $^{+}$ CD11b $^{+}$ CD86 $^{+}$  M1 phenotype in the ERC-Exo treated group was significantly lower than in the untreated group ( $P < 0.0001$ ). However, knocking out CD73 on ERC-Exo significantly increased the proportion of the M1 phenotype compared to the ERC-Exo-treated group ( $P < 0.05$ ). Furthermore, we also evaluated the F4/80 $^{+}$ CD11b $^{+}$ CD206 $^{+}$  M2 phenotype, as shown in Fig. 6C, D; the ERC-Exo treated group showed a high proportion of M2 phenotype ( $P < 0.0001$ ), while the knockout of CD73 attenuated the induction of the M2 phenotype ( $P < 0.0001$ ). Furthermore, immunofluorescence staining of renal macrophages also showed a significant increase in M2 markers (F4/80 and Arg-1) and a decrease in M1 markers (F4/80 and iNOS) after ERC-Exo treatment (Fig. 6E, F). In the CD73 $^{-/-}$ ERC-Exo-treated group, however, the proportion of M2 polarization was reversed compared to the ERC-Exo group. These data demonstrated that CD73 is vital for ERC-Exo-mediated M2 macrophage polarization and protection against renal I/R injury.

#### CD73 was a potential effector of ERC-Exo inhibiting proinflammatory polarization in primary BMDM in vitro

ERC-Exo facilitated the conversion of macrophages to the M2 phenotype and attenuated renal I/R injury; we next investigated whether CD73-expressing ERC-Exo affected macrophage polarization induced by LPS in vitro. PKH26-labelled exosomes were shown to be enriched in FITC-labelled F4/80 $^{+}$  BMDM cells (Fig. 7A), suggesting that BMDMs can take up exosomes, and the expression of CD73 in exosomes appeared to be independently associated with endocytosis. To investigate whether the modulatory effect of ERC-Exo on macrophage polarization correlates with CD73 expression, mice BMDM cells were isolated and co-cultured with Exo, CD73 $^{-/-}$ Exo, and CD73 $^{-/-}$ Exo + recombinant CD73(rCD73) in vitro. F4/80 $^{+}$ CD86 $^{+}$  cells and F4/80 $^{+}$ CD206 $^{+}$  cells were then selected as M1/M2 cell surface markers. As shown in Fig. 7B, C, the percentage of M1 cells in the LPS + Exo-treated group was significantly lower than in the LPS-treated group ( $P < 0.0001$ ) and lower than that in the LPS + CD73 $^{-/-}$ Exo-treated group ( $P < 0.01$ ). In particular, regarding the proportion of M1 cells in the LPS + CD73 $^{-/-}$ Exo, there was again a trend towards a lower proportion of M1 cells after the addition of rCD73 (CD73 $^{-/-}$ Exo group *vs.* CD73 $^{-/-}$ Exo + rCD73 group,  $P < 0.01$ ). Similarly, as shown in Fig. 7C, ERC-derived exosomes dramatically upregulated CD206 expression compared to those of the LPS-treated group ( $P < 0.01$ ). CD73 knockout abolished the effect of Exos on increasing M2 populations ( $P < 0.01$ ). The concentrations of M1-related iNOS and M2-related Arg-1 were also examined. As shown in Fig. 7D–F, ERC-Exo inhibited LPS-induced iNOS generation and enhanced Arg-1 expression (LPS group *vs.* LPS + Exo group: iNOS,  $P < 0.001$ ; Arg-1,  $P < 0.0001$ ). In contrast, in the LPS + CD73 $^{-/-}$ Exo-treated group, the regulatory effect of ERC-Exo was significantly weakened (LPS + Exo group *vs.* LPS + CD73 $^{-/-}$ Exo group: iNOS,  $P < 0.05$ ; Arg-1,  $P < 0.001$ ). These results suggested that CD73-mediated ERC-Exo could convert the macrophage phenotype from a proinflammatory M1 to an anti-inflammatory M2.

(See figure on next page.)

**Fig. 3** CD73-positive Exo released by ERC alleviate renal dysfunction and pathologic injury in renal I/R mice. Briefly, mice were concurrently treated with ERC-Exo and CD73 $^{-/-}$ ERC-Exo every 24 h after renal I/R injury and were euthanized at 3 days after disease induction. **A** Imaging of fluorescence intensity of indicated organs at 12 h after injection (40 min ischemic time). **B** Representative kidney histology of H&E staining of renal cortex and medulla (scale bar: 100  $\mu$ m). **C** Analysis of tubular injury score ( $n = 6$ ). **D** and **E** Representative images of TUNEL staining and quantification of the apoptotic cells (Scale bars: 50  $\mu$ m. HFP, High power field) ( $n = 6$ ). **F** Serum creatinine (sCr) concentration in different groups of mice after renal I/R ( $n = 6$ ). **G** Blood urea nitrogen (BUN) levels of different groups of mice after renal I/R ( $n = 6$ ). **H** Cell viability in HK-2 cells after treated with H/R and ERC-Exo and CD73 $^{-/-}$ ERC-Exo was measured by CCK-8 kits ( $n = 5$ ). Data are presented as mean  $\pm$  s.e.m (SEM). ns, no significance; \* $P < 0.05$ ; \*\*\* $P < 0.001$ ; \*\*\*\* $P < 0.0001$ , analyzed by one-way ANOVA with Tukey's multiple comparison post hoc test

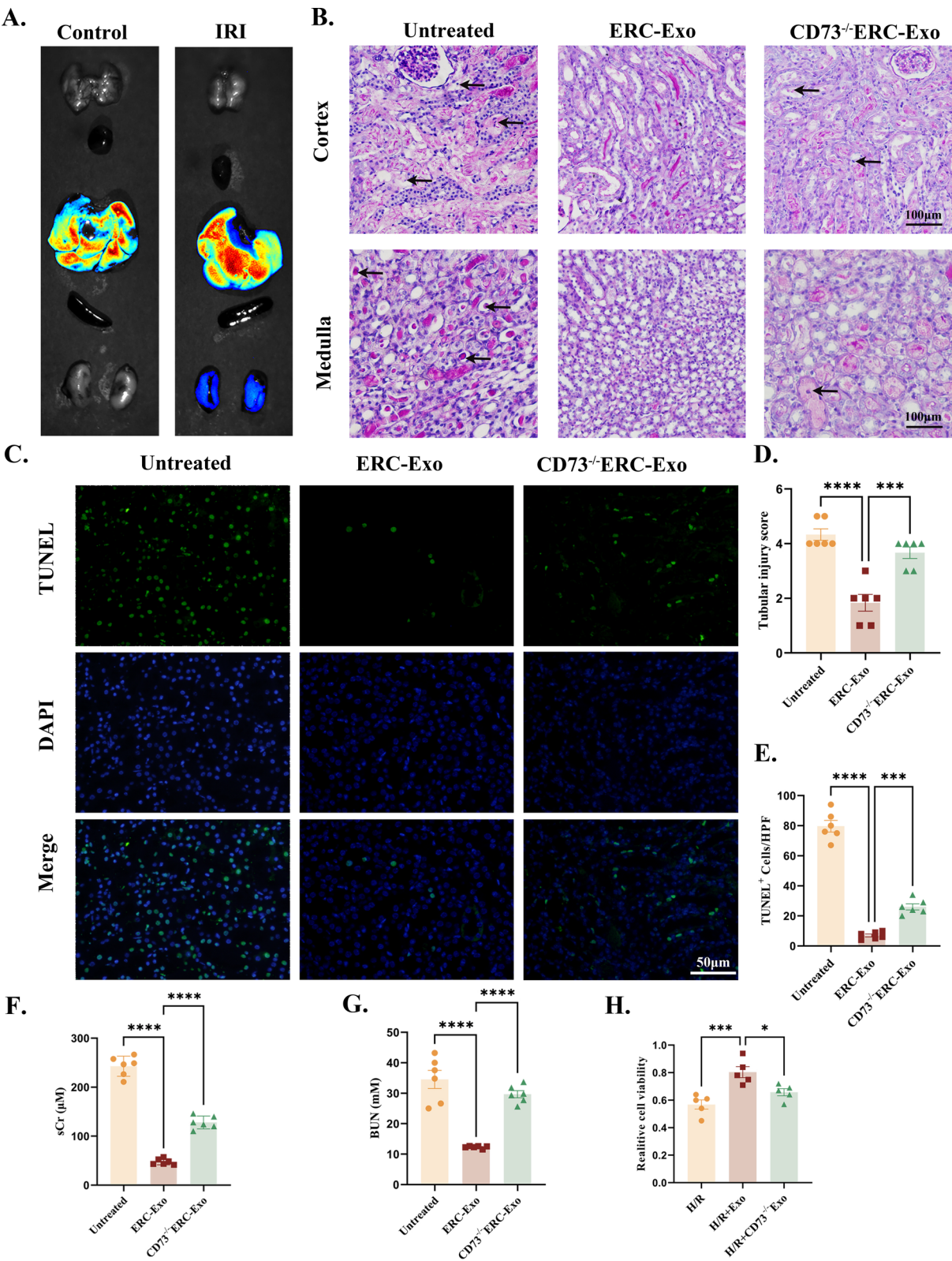


**Fig. 3** (See legend on previous page.)

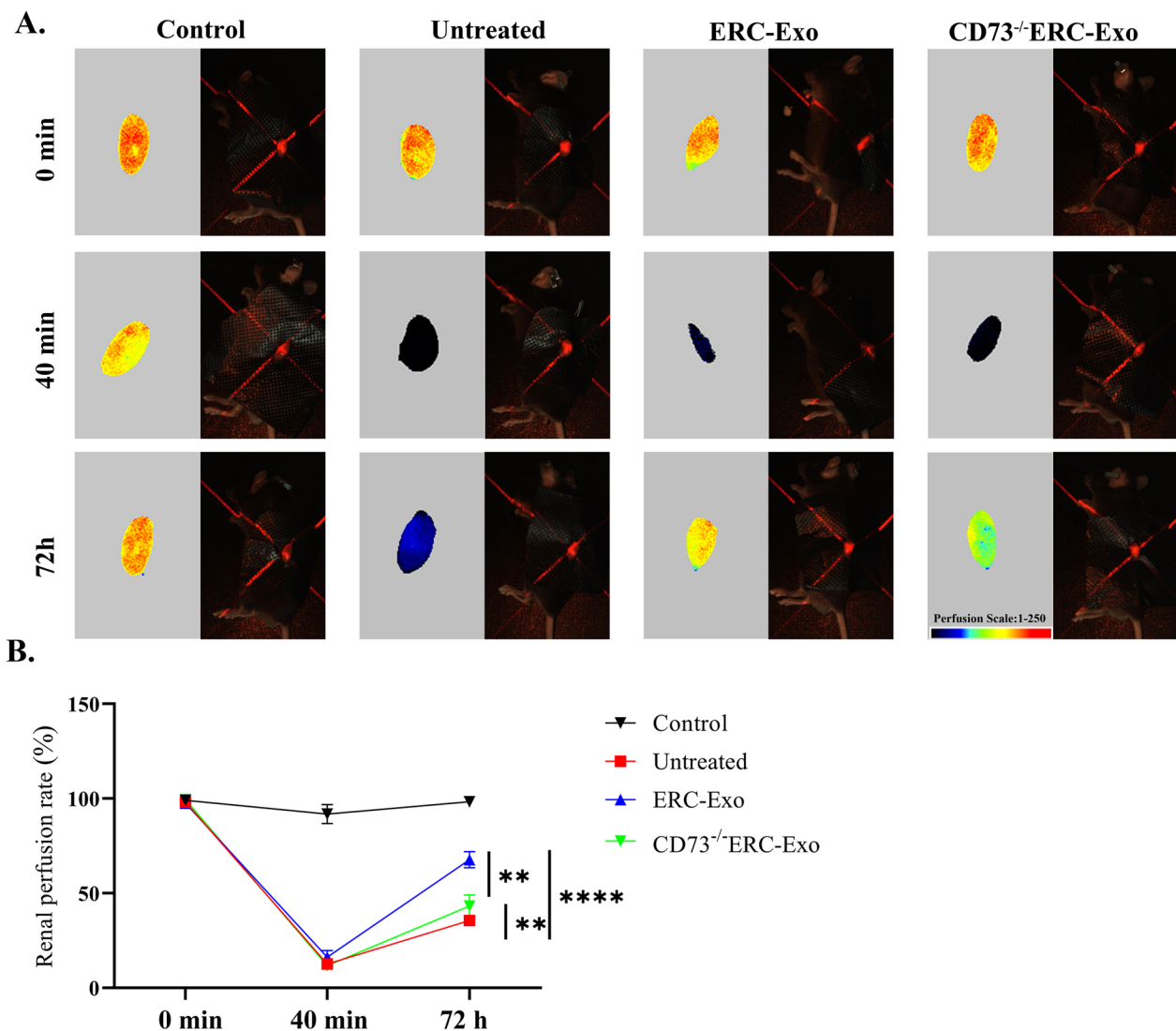


**Fig. 4** CD73-positive Exo restored impaired renal blood flow in renal I/R mice. **A** Representative Laser Doppler images obtained by scanning mouse kidneys in three different groups. For each group, images are shown before ischaemic insult (0), after 40 min of ischaemia (40 min) and after 72 h of reperfusion (72 h). For each group, both colour laser Doppler images (left) showing renal blood flow and phase contrast images (right) showing the morphology of the kidneys at each time point were shown. A colour scale shows the variations in renal blood flow from minimal flow (dark blue) to high flow (red). **B** Statistics of renal perfusion rates from laser Doppler images at baseline, after 40 min of ischaemia and after 72 h of reperfusion (n = 5). Data are presented as mean ± s.e.m (SEM). \*\*P < 0.01; \*\*\*\*P < 0.0001, analyzed by one-way ANOVA with Tukey's multiple comparison post hoc test

(See figure on next page.)

**Fig. 5** CD73-positive Exo released by ERC regulates CD4<sup>+</sup>T cell differentiation in renal I/R mice. Immune cells were freshly isolated from the kidney on day 3 after renal I/R. To identify Th1 and Th17 cells, kidney mononuclear cells were first incubated with a stimulation cocktail for 5 h, followed by staining with a fluorescent antibody. Flow cytometry plots and graph analysis of CD4<sup>+</sup>IFN-γ<sup>+</sup> Th1 (**A**), CD4<sup>+</sup>IL-17<sup>+</sup>Th17 (**C**), and CD4<sup>+</sup>CD25<sup>+</sup>Foxp3<sup>+</sup>Tregs (**E**) in the kidneys from the Untreated, ERC-Exo and CD73<sup>-/-</sup>ERC-Exo-treated groups. Percentage of CD4<sup>+</sup>IFN-γ<sup>+</sup>Th1 (**B**), CD4<sup>+</sup>IL-17<sup>+</sup>Th17 cells (**D**) and CD4<sup>+</sup>CD25<sup>+</sup>Foxp3<sup>+</sup>Tregs (**F**) (n = 5). **G–J** The ELISA results of TNF-α, IL-6, IL-1β, and IL10 of kidney homogenates (n = 6). Data are presented as mean ± s.e.m (SEM). ns, no significance; \* P < 0.05; \*\*P < 0.01; \*\*\*P < 0.001; \*\*\*\*P < 0.0001, analyzed by one-way ANOVA with Tukey's multiple comparison post hoc test



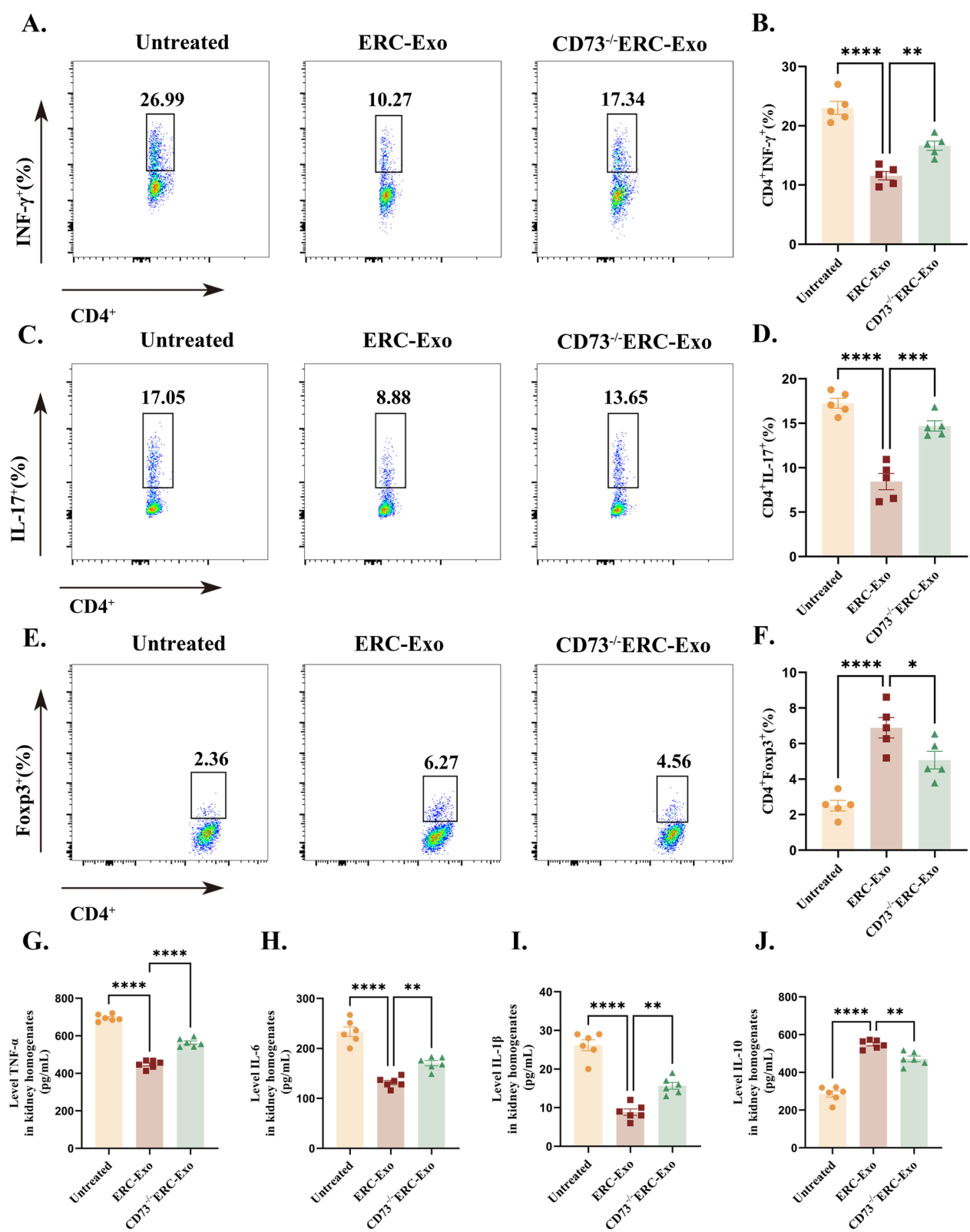


**Fig. 5** (See legend on previous page.)

### ERC-Exosomal CD73 improved macrophage immunoregulatory function associated with the p38/ERK1/2 signaling pathway

We investigated the immunoregulatory ability of macrophages to induce CD4<sup>+</sup>T differentiation to Treg cells with a co-culture system. As illustrated in Fig. 8A, B, the proportion of CD4<sup>+</sup>Foxp3<sup>+</sup> Tregs was significantly increased in the LPS+Exo group compared with the LPS group ( $P < 0.0001$ ), while the knockout of CD73 reduced the induction of Tregs (LPS+Exo group vs. LPS+CD73<sup>-/-</sup>Exo group,  $P < 0.01$ ). In particular, there was again a trend towards a higher proportion of Treg cells after the addition of rCD73 in the LPS+CD73<sup>-/-</sup>Exo group (CD73<sup>-/-</sup>Exo group vs. CD73<sup>-/-</sup>Exo+rCD73 group,  $P < 0.05$ ). In addition, ERC-exosomal CD73 decreased the levels of IL-1 $\beta$ , IL-6, and TNF- $\alpha$  while increasing the levels of IL-10 (Fig. 8C–F), indicating its ability to inhibit the activation of proinflammatory cells.

The mitogen-activated protein kinase (MAPK) signaling pathway, including extracellular signal-regulated kinase 1/2 (ERK1/2) and p38, is essential for macrophage polarization [23]. Several studies have demonstrated that the MAPK pathway was activated during proinflammatory macrophage polarization and that inhibiting this pathway could convert the macrophage phenotype from a proinflammatory M1 to an anti-inflammatory M2 [24, 25]. We assessed the phosphorylation of MAPK pathway-related proteins in proinflammatory polarized BMDM cells. Specifically, as shown in Fig. 8G–I, ERC-Exo inhibited LPS-dependent phosphorylation of p38 and ERK1/2, whereas there were no differences in the expression of total p38 and ERK1/2 in primary BMDM (LPS+Exo group vs. LPS group: p-P38,  $P < 0.0001$ ; p-ERK1/2,  $P < 0.0001$ ). In contrast, the contribution of ERC-Exo was significantly impaired by CD73 knockout (LPS+CD73<sup>-/-</sup>Exo group vs. LPS+Exo group: p-P38,  $P < 0.001$ ; p-ERK1/2,  $P < 0.01$ ). Together, these results demonstrated that activation of the MAPK pathway was suppressed by CD73-expressing ERC-Exo in proinflammatory polarized primary BMDM.

### Discussion

Ischaemic AKI due to surgical renal ischemia (e.g., kidney transplant, part nephrectomy) or renal hypoperfusion (e.g., due to aortic surgery, cardiogenic shock, or sepsis) is a prominent cause of AKI [26]. Renal I/R contributes to AKI caused by renal tubular necrosis during ischemia and severe inflammatory insults caused by free radicals and infiltrating proinflammatory leukocytes during reperfusion [27]. Stem cell therapy with MSC has attracted considerable interest, with one clinical trial demonstrating that emerging stem cell therapies may represent the predominant therapy for AKI [28]. Adipose-derived mesenchymal stem cells (ADMSC) and bone marrow mesenchymal stem cells (BMMSC) had to be obtained by invasive methods. In contrast, umbilical cord-derived mesenchymal stem cells (UCMSC) were difficult to autologously transplant due to their immunogenicity [29]. ERC, as a type of therapeutic stem cell, not only retains all the properties of MSC but also shows more advantageous characteristics in clinical application due to their completely non-invasive harvesting process and almost unrestricted periodic collection [30]. Exosomes derived from the ERC have shown excellent therapeutic effects in several diseases, including fulminant hepatic failure [31], premature ovarian insufficiency [32], and cardiac allograft rejection [33]. Although MSCs derived from endometrial blood have been well investigated in the literature, we are concerned with the study of the mechanisms by which exosomes improve renal I/R injury. As an emerging science developed in recent years, exosomes have shown great advantages in disease treatment and targeted drug delivery. The molecular mechanism by which ERC-Exo improve the renal immune microenvironment in renal I/R injury remains unclear.

In the present study, we first identified CD73 expression in ERC-Exo. Our results demonstrated that ERC-Exo were a potent candidate for renal I/R, providing a local CD73<sup>+</sup>Exo environment in the inflammatory process, which macrophages took up to facilitate the formation of an immunosuppressive niche. ERC-exosomal CD73 effectively attenuated renal function, protein casts, necrosis, and detachment of TECs. Impressively, ERC-exosomal CD73 significantly reduced the populations of Th1 and Th17 cells but increased the proportion of Tregs in the

(See figure on next page.)

**Fig. 6** CD73-positive Exo released by ERC induces a shift in renal macrophages. Exploration of the phenotype changes of renal macrophages from the Untreated, ERC-Exo, and CD73<sup>-/-</sup>ERC-Exo-treated groups. Flow cytometry analysis of F4/80<sup>+</sup>CD86<sup>+</sup> (A) or F4/80<sup>+</sup>CD206<sup>+</sup> (B) macrophages in the kidneys. Percentage of F4/80<sup>+</sup>CD86<sup>+</sup> (C) or F4/80<sup>+</sup>CD206<sup>+</sup> (D) macrophages in the kidneys (n=6). (E) Representative immunofluorescence images of F4/80<sup>+</sup>iNOS<sup>+</sup> or F4/80<sup>+</sup>Arg-1<sup>+</sup> macrophages in kidney sections (n=5) (Scale bars: 25  $\mu$ m). M1-like (iNOS) and M2-like (Arg-1) markers indicated the shift of macrophages. Data are presented as mean  $\pm$  s.e.m (SEM). ns, no significance; \* $P < 0.05$ ; \*\*\*\* $P < 0.0001$ , analyzed by one-way ANOVA with Tukey's multiple comparison post hoc test

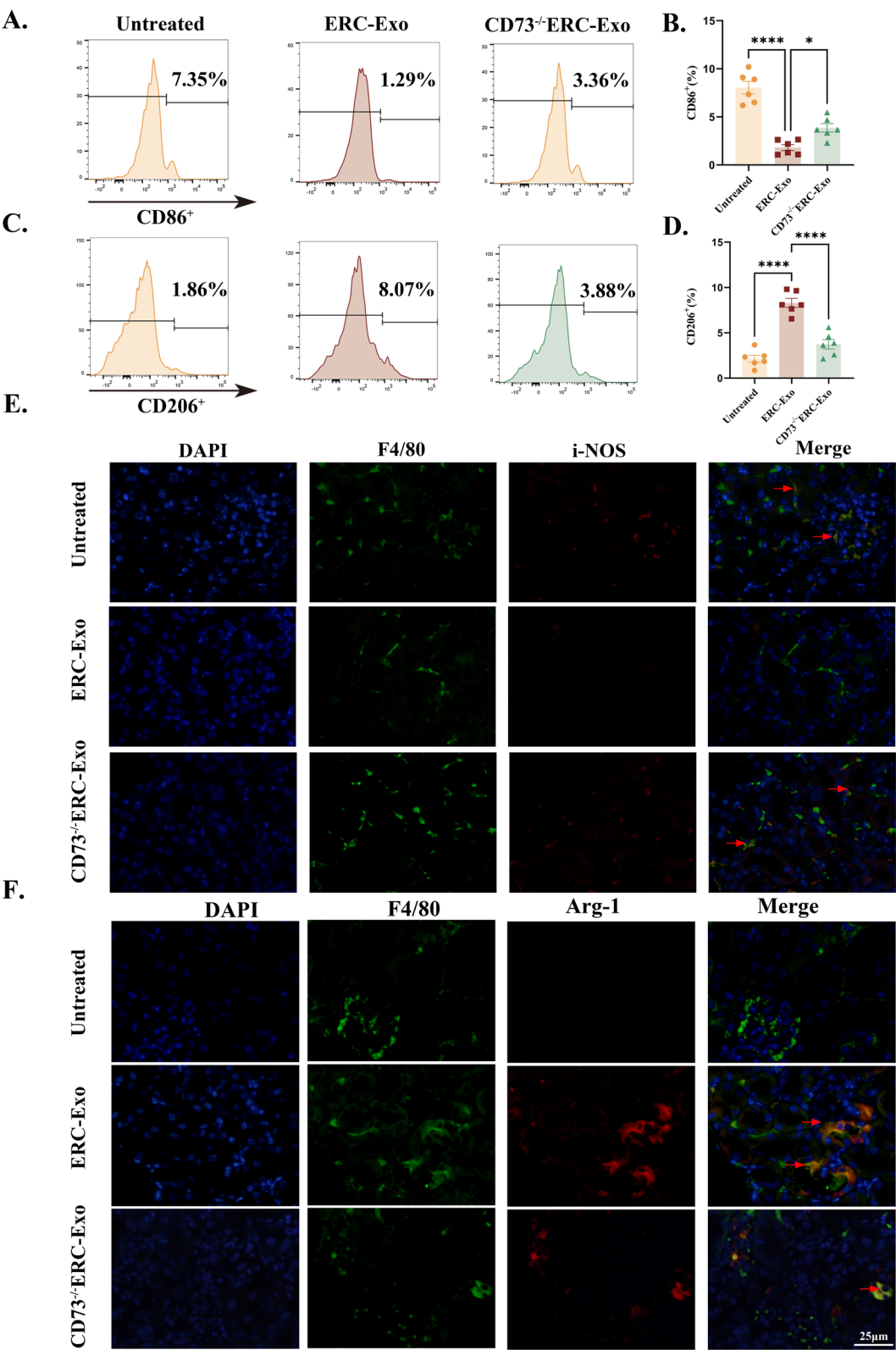


**Fig. 6** (See legend on previous page.)

renal immune microenvironment. Additionally, ERC-exosomal CD73 significantly reduced levels of proinflammatory cytokines (IL-1 $\beta$ , IL-6, TNF- $\alpha$ ) and increased levels of anti-inflammatory cytokines (IL-10) in the kidney. Significantly, ERC-exosomal CD73 suppressed the proinflammatory M1 polarization and improved the anti-inflammatory M2 polarization in vivo and in vitro. We demonstrated that such effects were mainly achieved associated with the MAPK pathway (including ERK and p38 pathways). Collectively, these data provided insight into the mechanisms by which ERC-Exo facilitated the hydrolysis of proinflammatory ATP to immunosuppressive ADO via CD73, which may be involved in the regulation of innate immune responses, and exerted efficient therapeutic efficacy against renal I/R injury.

CD73, as a phenotypic marker of ERC, is attributed to restorative and immunomodulatory properties. Local inflammation can be reduced, and tissue regeneration can be facilitated by ADO, which is derived from the dephosphorylation activity of CD73 [34]. For example, CD73<sup>-/-</sup> mice developed significantly more severe renal tubular destruction. They exhibited unresolved inflammation, suggesting that treatment with soluble CD73-dependent adenosine production may be a novel therapeutic approach for treating renal diseases triggered by limited oxygen availability [35]. The AMPase CD73 is often present in modulatory EVs, a rate-limiting enzyme in the extracellular purine metabolic pathway that coordinates the critical homeostatic balance of extracellular adenosine levels [36]. Its enzymatic activity is closely related to extracellular phosphatase (CD39), which produces AMP, which is a substrate for the action of CD73. MSCs express high levels of CD73, and this is reflected in the corresponding EVs. The package of CD73 in EVs from other kind of MSCs e.g., umbilical cord, bone marrow, urethral tissues, and gingiva [37–40]. Zhai et al. demonstrated that CD73-containing MSC-extracellular vesicles from umbilical cord ameliorated inflammation after spinal cord injury by reducing extracellular ATP, promoting the A<sub>2B</sub>R/PKA pathway [37]. CD73-positive MSC-sEVs from urethral tissues further promoted angiogenesis by activating A<sub>2A</sub>R [39]. TNF- $\alpha$ -enhanced gingival tissue-derived MSCs (GMSCs) exosomal CD73 expression

contributed to M2 macrophage polarization and inhibit periodontal bone loss [38]. In experimental autoimmune uveitis, overexpression of CD73 on MSC-sEVs enhanced their immunosuppressive effects [40]. As a type of therapeutic stem cells, we showed that CD73-containing ERC-exosome also played an essential role in the immunomodulatory effects. Our in vivo experiments showed that proinflammatory M1 polarization, Th1, and Th17 cells were reduced by naive Exo but reversed by CD73-silenced ERC-Exo. Furthermore, the phenotype and size of CD73<sup>-/-</sup>ERC-Exo were not altered by transfection.

ADO, catalytically produced by CD73, exert a highly immunosuppressive effect interacting with adenosine receptors on a variety of immune cells, both T cells and macrophages [41, 42]. However, macrophages are phagocytic innate immune cells that are important mediators of tissue homeostasis and host defense. Classically activated macrophages contribute to the development of renal I/R injury [43]. Macrophages, a type of highly heterogeneous innate immune cell, are initially polarized into the proinflammatory subtype under the stimulation of various injury factors released in renal I/R injury and release more inflammatory cytokines to contribute to and amplify the damage caused by renal I/R injury [43]. Many studies have shown that manipulating macrophage infiltration and polarization can significantly improve the prognosis of early acute injury and late fibrosis in I/R kidneys [44–46]. Mao, R et al. observed that peritoneal M2 macrophages ameliorated renal I/R by decreasing inflammatory response and promoting primary proximal tubular epithelial cell proliferation [47]. Vinuesa E. et al. identified the association between alternative activation of macrophages and renal regeneration after ischemia/reperfusion [48]. Moreover, Huang, J et al. showed that inflammation after hUC-MSC exosomes inhibited renal I/R promoted M2 polarization [49]. Traditionally, macrophages can be manipulated to the M2 phenotype to treat AKI.

Interestingly, our research also revealed that ERC-exosomal CD73 had the ability to disrupt macrophage polarization. We found that ERC exosomes mediated M2 macrophage polarization by catalyzing the production of ADO from AMP through CD73 expressed on the surface

(See figure on next page.)

**Fig. 7** CD73 enriched in Exo from ERC contributed to M2 polarization in vitro. **A** Representative fluorescence microscope showing uptake of PKH26-labeled exosomes (red) by BMDMs (green, F4/80<sup>+</sup>), counterstained by DAPI (blue) (Scale bars: 25  $\mu$ m). **B, C** Macrophage surface markers, CD86 for M1 and CD206 for M2, on M1 that were treated with ERC-Exo, CD73<sup>-/-</sup>ERC-Exo, or rCD73 for 24 h were examined by using flow cytometry (n = 3). **D–F** Macrophage intracellular markers, iNOS for M1 and Arg-1 for M2, in M1 that were treated with the indicated concentration of ERC-Exo, CD73<sup>-/-</sup>ERC, or rCD73 for 24 h were examined by using immunoblotting with GAPDH as a loading control (n = 3). Full-length blots/gels are presented in Additional file 1: Fig. S3. Data are presented as mean  $\pm$  s.e.m (SEM). ns, no significance; \* $P$  < 0.05; \*\* $P$  < 0.01; \*\*\* $P$  < 0.001; \*\*\*\* $P$  < 0.0001, analyzed by one-way ANOVA with Tukey's multiple comparison post hoc test



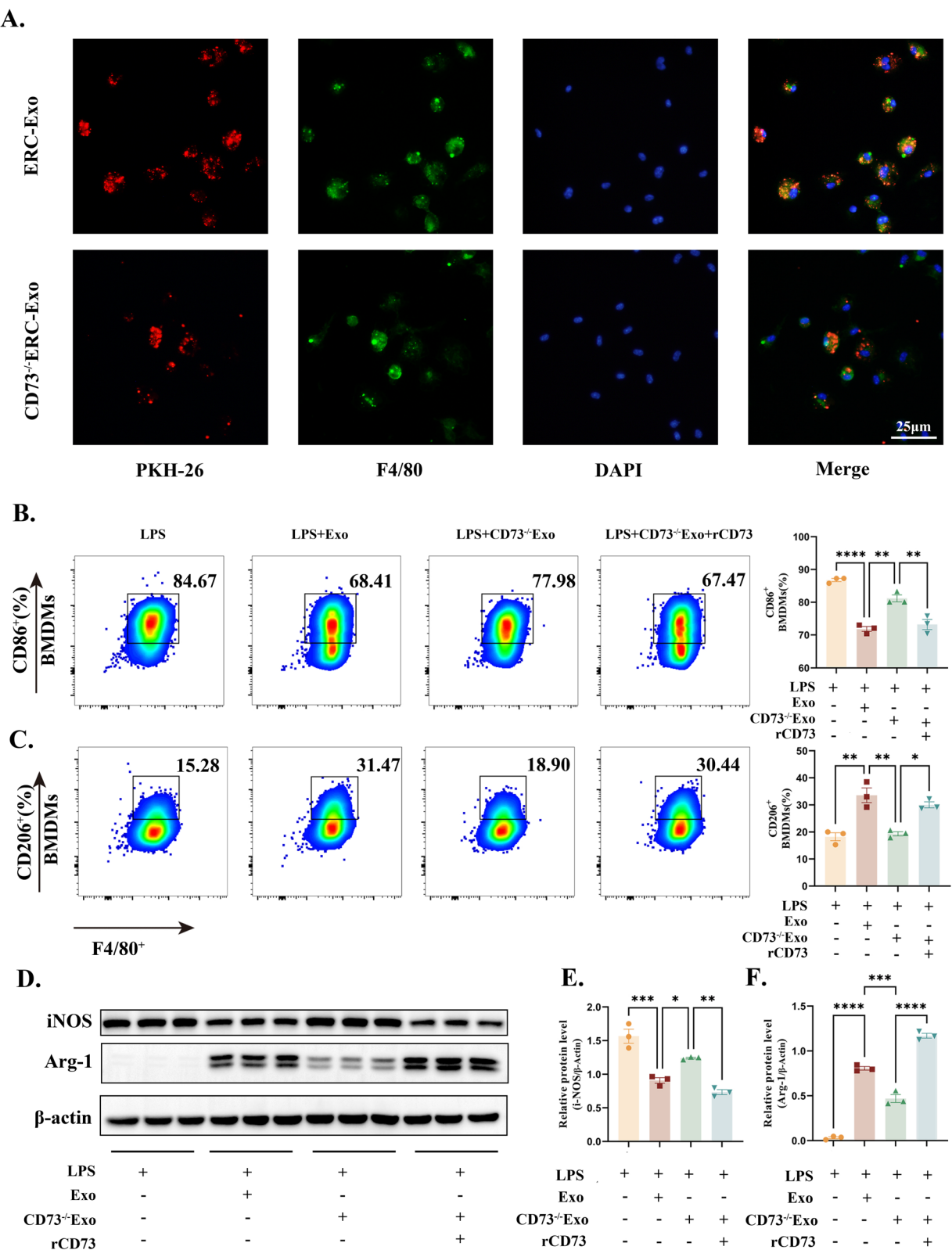


**Fig. 7** (See legend on previous page.)

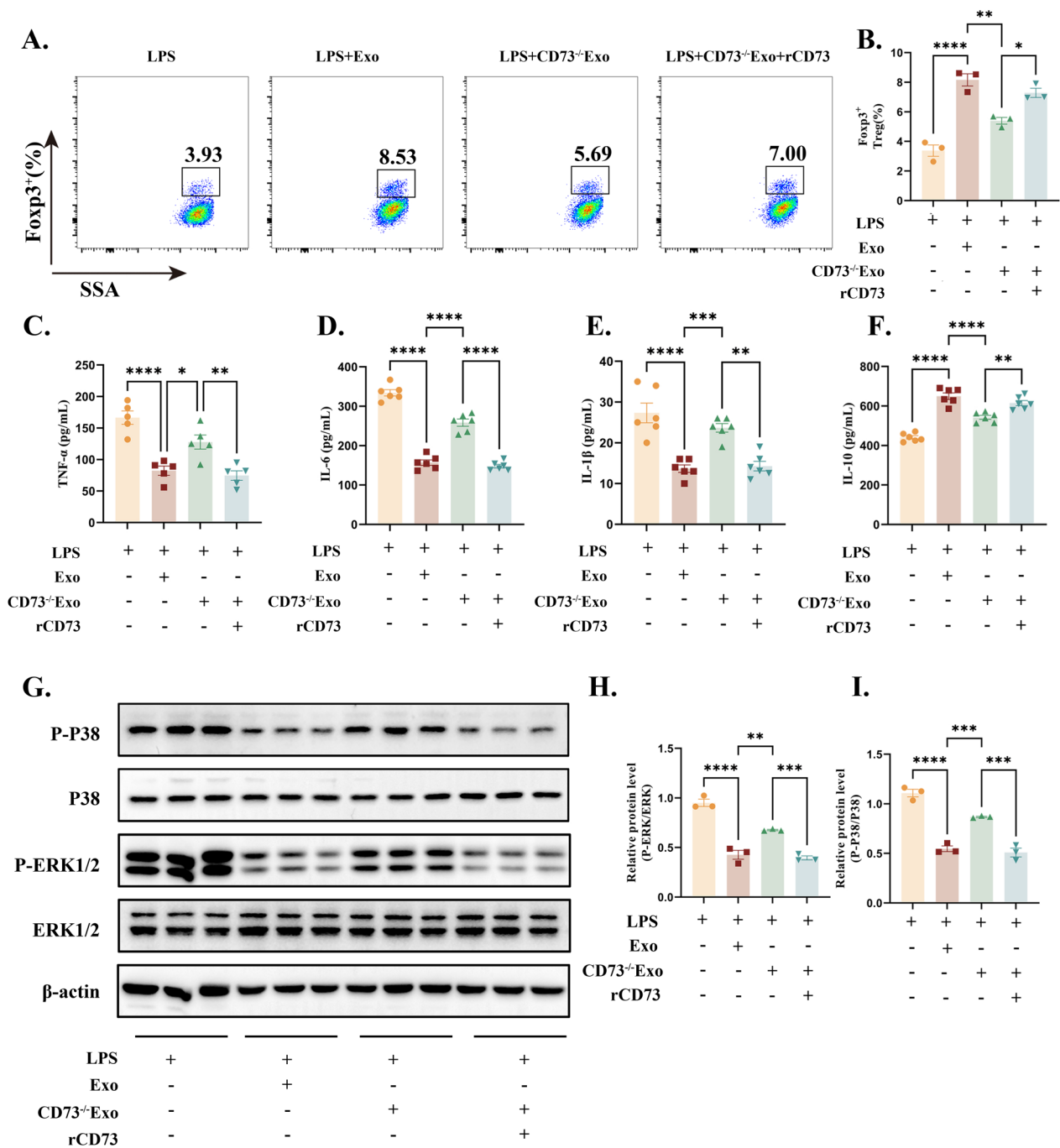


**Fig. 8** CD73 enriched in Exo from ERC contributed to M2 polarization associated with the MAPK pathway in vitro. **A, B** The representative pseudocolor plots of Foxp3<sup>+</sup> T cells were depicted in vitro (n = 3). **C–F** The IL-6, IL-1 β, TNF-α, and IL-10 were examined in the supernatant (n = 6). **G–I** To explore whether the MAPK pathway would participate in M2 polarization and activation mediated by CD73-positive Exo released by ERC in vitro, western blot was used to determine p-P38 and P38, p-ERK1/2 and ERK1/2 with GAPDH as a reference (n = 3). Full-length blots/gels are presented in Additional file 1: Fig. S4. Data are presented as mean ± s.e.m (SEM). ns, no significance; \*P < 0.05; \*\*P < 0.01; \*\*\*P < 0.001; \*\*\*\*P < 0.0001, analyzed by one-way ANOVA with Tukey's multiple comparison post hoc test

of ERC exosomes. Consistent with our observations, several studies have reported that ADO, which exerted an anti-inflammatory effect, inhibited the production of proinflammatory cytokines by macrophages. In particular, ADO could bind to four ADO receptors: A1, A<sub>2A</sub>, A<sub>2B</sub>, and A3 receptors [50]. In many reports, macrophage

polarization has been shown to be modulated by ADO receptor subtypes. For example, ADO was reported to enhance IL-4 and IL-13-induced M2 macrophage polarization via the A<sub>2A</sub> receptor and, to a lesser extent, the A<sub>2B</sub> receptor [51].

Furthermore, activating the A<sub>2A</sub> receptor also increased macrophage production of the anti-inflammatory cytokine IL-10 [52]. While A1 and A3 receptors combine with G-protein subtype Gi to inhibit adenylate cyclase (AC) and reduce cyclic AMP (cAMP) production, A<sub>2A</sub> and A<sub>2B</sub> receptors combine with G-protein subtype Gs and activate AC, increasing cAMP production [53]. Elevated cAMP levels reportedly promoted M2 macrophage polarization. We infer that CD73<sup>+</sup>Exo may increase the concentration of ADO in the inflammatory microenvironment through AMP and ATP dephosphorylation. Under high ADO conditions in the inflammatory microenvironment, macrophages increase intracellular cAMP levels by activating A<sub>2A</sub> and A<sub>2B</sub> receptors to induce M2 polarization and inhibit the production of proinflammatory cytokines. Therefore, the receptor of ERC-exosomal CD73 acting on macrophages needs to be further investigated in vitro and animal experiments.

Mitogen-activated protein kinase (MAPK) signaling is a major macrophage polarization and inflammation pathway, implicating ERK and p38 [54]. External stress signals are transmitted to the nucleus via activation of the MAPK pathway, which is required for M1 macrophage polarization, and inhibition of this pathway may prevent M1 macrophage polarization and promote M1–M2 polarization [55]. To determine the upstream activator of ERK and p38 phosphorylation, we proposed CD73 as a likely candidate, as it is abundant and enzymatically active in the ERC exosome. It is also the only extracellular ecto-5'-nucleotidase known to degrade extracellular AMP to ADO, which in turn can induce pro-survival ERK and p38 signaling through interaction with the adenosine receptor [56]. MSC exosomes have been shown to activate ERK1/2 phosphorylation in macrophages via ADO receptor signaling in the presence of AMP [57]. Sun, Z. et al. found that when BMDM were exposed to titanium particles, CD73 enhanced M2 polarization via the p38 pathway [58]. This study showed that CD73-containing exosomes suppressed the phosphorylation of ERK1/2 and p38 signaling in LPS-stimulated BMDM cells (M1 phenotype) and enhanced the polarization of macrophages to the M2 phenotype in vitro. Cascading proinflammatory cytokines such as IL-1 $\beta$ , IL-6, and TNF- $\alpha$  were downregulated, while anti-inflammatory cytokine such as IL-10 was upregulated. Other studies also showed that CD73 promoted M2 macrophage polarization through activation of PKA-mediated signaling pathways such as AKT [59] and STAT3 [60]. Therefore, other pathways

may mediate the effects of CD73-containing ERC-Exo in M2-like macrophage polarization.

ERC-Exo represent an exciting future avenue for development of therapeutics in renal I/R injury. Our current research is still in pre-clinical studies and has not yet reached the clinical stage. As an emerging science that has developed over the last few years, there are no “mutant” EVs for clinical application. However, a limited number of clinical trials have confirmed the safety and efficacy of MSC-EVs in the treatment of disease, such as rheumatoid arthritis and severe COVID-19 [61–63]. Future research should aim to use modern techniques for reliable ERC-Exo isolation and multimodal characterization, to develop efficient methods for producing, storing and delivering ERC-Exo, and to design innovative studies that will enable clinical translation. Despite these challenges, this field represents a great opportunity to translate the ERC-Exo potential as therapeutics and as vehicles for drug delivery to improve renal function.

## Conclusion

This study demonstrated that ERC-Exo were preferential to attenuate renal I/R injury by inducing a polarization shift of macrophages towards an anti-inflammatory phenotype. CD73 is a critical modulator of the MAPK signaling pathway. These findings highlight the therapeutic potential of ERC-Exo in renal I/R injury and demonstrate the significance of CD73 in regulating macrophage polarization. In the future, more research using different models and conditions, as well as confirmation by clinical trials or in vitro experiments using human samples, will be needed to improve the applicability of our findings.

## Abbreviations

AKI	Acute kidney injury
I/R	Renal ischemia–reperfusion
MSC	Mesenchymal stromal cells
ERC	Endometrial regenerative cells
NT5E	Ecto-5'-nucleotidase
ADO	Adenosine
ATP	Adenosine triphosphate
TEM	Transmission electron microscopy
HE	Hematoxylin–eosin
NTA	Nanoparticle tracking analysis
BMDMs	Bone marrow derived macrophages
TEM	Transmission electron microscope
NTA	Nanoparticle tracking analysis
MAPK	Mitogen-activated protein kinase
IFN- $\gamma$	Interferon- $\gamma$
ERK1/2	Extracellular signal-regulated kinase 1/2
AC	Adenylate cyclase

## Supplementary Information

The online version contains supplementary material available at <https://doi.org/10.1186/s13287-025-04275-9>.

Additional file 1: Figure S1–Figure S4. The full uncropped Gels and Blots image(s).

Additional file 2: he ARRIVE guidelines 2.0.

Additional file 3: Supplementary Figure S1. CD73-positive Exo released by ERC inhibited the splenocytes proliferation. (A–C) The representative contour plots were depicted. (D) The proliferation of the splenocytes was measured by CCK-8. (E–G) show the statistical graph. Data are presented as mean  $\pm$  s.e.m (SEM). ns, no significance; \* $P < 0.05$ ; \*\* $P < 0.01$ ; \*\*\* $P < 0.001$ , analyzed by one-way ANOVA with Tukey's multiple comparison post hoc test.

## Acknowledgements

We would like to thank all college's that contributed to this project. The authors declare that artificial intelligence is not used in this study.

## Author contributions

Bo Shao: conception and design, collecting and assembling data, analyzing and interpreting data, writing manuscripts; Hong-da Wang and Shao-hua Ren: collecting and assembling data, data analysis, and interpretation, writing manuscripts; Qiang Chen, Zhao-bo Wang, Yi-ni Xu, Tong Liu, Cheng-lu Sun, Yi-yi Xiao, Hong-yu Jiang, Yi-cheng Li, Peng-yu Zhao, Guang-mei Yang, Xu Liu and Yu-fan Ren: collecting and assembling data, data analysis, and interpretation; Hao Wang: conception and design, administrative support, financial support, manuscript writing and final approval of the manuscript. All authors have read and agreed to the final content of this manuscript.

## Funding

This work was supported by grants to Hao Wang from the National Natural Science Foundation of China (No. 82071802 and 82270794), Natural Science Foundation of Tianjin (No. 21JCYBJC00850), Science and Technology Project of Tianjin Health Commission (No. TJWJ2021MS004), and Tianjin Key Medical Discipline (Specialty) Construction Project (TJYXZDXK-076C).

## Availability of data and materials

All data generated or analysed during this study are included in this published article and its supplementary information files.

## Declarations

### Ethics approval and consent to participate

This study was performed following the Declaration of Helsinki Ethical Principles and approved by the Ethics Committee of the Tianjin Medical University General Hospital, Tianjin, China (Approval number: IRB2024-YX-014–01). (1) Title of the approved project: Studies on the mechanism of human menstrual blood-derived endometrial regenerative cell exosomes in the therapy of ischaemia–reperfusion. (2) Name of the institutional approval committee: the Ethics Committee of the Tianjin Medical University General Hospital, Tianjin, China. (3) Approval number: IRB2024-YX-014–01. (4) Date of approval: 01/25/2024. After filling out the informed consent letter, All human menstrual blood samples were obtained from Tianjin Medical University General Hospital from healthy female volunteers (20–30 years of age). The animal care and experimental protocols were approved by the Institutional Animal Care and Use Committee of Tianjin Medical University General Hospital and was conducted in accordance with the ARRIVE guidelines 2.0 (Project title: Studies on the mechanism of human menstrual blood-derived endometrial regenerative cell exosomes in the therapy of ischaemia–reperfusion; Approval number: IRB2024-DW-08; Date of approval: 01/30/2024).

### Consent for publication

Not applicable.

### Competing interest

No potential conflict of interest was reported by the author(s).

### Author details

<sup>1</sup>Department of General Surgery, Tianjin Medical University General Hospital, 154 Anshan Road, Heping District, Tianjin 300052, China. <sup>2</sup>Tianjin General Surgery Institute, Tianjin Medical University General Hospital, Tianjin, China. <sup>3</sup>Tianjin Key Laboratory of Precise Vascular Reconstruction and Organ Function

Repair, Tianjin, China. <sup>4</sup>Department of General Surgery, The Affiliated Hospital of Inner Mongolia Medical University, Hohhot, China.

Received: 14 January 2025 Accepted: 11 March 2025

Published online: 26 March 2025

## References

- Chawla LS, Bellomo R, Bihorac A, Goldstein SL, Siew ED, Bagshaw SM, Bittleman D, Cruz D, Endre Z, Fitzgerald RL, Forni L, Kane-Gill SL, Hoste E, Koyner J, Liu KD, Macedo E, Mehta R, Murray P, Nadim M, Ostermann M, Palevsky PM, Pannu N, Rosner M, Wald R, Zarbock A, Ronco C, Kellum JA. Acute kidney disease and renal recovery: consensus report of the acute disease quality initiative (ADQI) 16 Workgroup. *Nat Rev Nephrol*. 2017;13(4):241–57. <https://doi.org/10.1038/nrneph.2017.2>.
- Lin Y, Manning PT, Jia J, Gaut JP, Xiao Z, Capoccia BJ, Chen CC, Hiebsch RR, Upadhyay G, Mohanakumar T, Frazier WA, Chapman WC. CD47 blockade reduces ischemia-reperfusion injury and improves outcomes in a rat kidney transplant model. *Transplantation*. 2014;98(4):394–401. <https://doi.org/10.1097/TP.0000000000000252>.
- Fazekas B, Griffin MD. Mesenchymal stromal cell-based therapies for acute kidney injury: progress in the last decade. *Kidney Int*. 2020;97(6):1130–40. <https://doi.org/10.1016/j.kint.2019.12.019>.
- Cordeiro MR, Carvalhos CA, Figueiredo-Dias M. The emerging role of menstrual-blood-derived stem cells in endometriosis. *Biomedicine*. 2022. <https://doi.org/10.3390/biomedicine11010039>.
- Meng X, Ichim TE, Zhong J, Rogers A, Yin Z, Jackson J, Wang H, Ge W, Bogin V, Chan KW, Thebaud B, Riordan NH. Endometrial regenerative cells: a novel stem cell population. *J Transl Med*. 2007;5:57. <https://doi.org/10.1186/1479-5876-5-57>.
- Oh Y, Qin H, Hong C, Blouin L, Polo JM, Guo T, Qi Z, Downey SL, Manos PD, Rossi DJ, Yu J, Hebrok M, Hochedlinger K, Costello JF, Song JS, Ramalho-Santos M. Incomplete DNA methylation underlies a transcriptional memory of somatic cells in human iPS cells. *Nat Cell Biol*. 2011;13(5):541–9. <https://doi.org/10.1038/ncb2239>.
- Karnoub AE, Dash AB, Vo AP, Sullivan A, Brooks MW, Bell GW, Richardson AL, Polyak K, Tubo R, Weinberg RA. Mesenchymal stem cells within tumour stroma promote breast cancer metastasis. *Nature*. 2007;449(7162):557–63. <https://doi.org/10.1038/nature06188>.
- Zhou C, Zhang B, Yang Y, Jiang Q, Li T, Gong J, Tang H, Zhang Q. Stem cell-derived exosomes: emerging therapeutic opportunities for wound healing. *Stem Cell Res Ther*. 2023;14(1):107. <https://doi.org/10.1186/s13287-023-03345-0>.
- He J, Ao C, Li M, Deng T, Zheng S, Zhang K, Tu C, Ouyang Y, Lang R, Jiang Y, Yang Y, Li C, Wu D. Clusterin-carrying extracellular vesicles derived from human umbilical cord mesenchymal stem cells restore the ovarian function of premature ovarian failure mice through activating the PI3K/AKT pathway. *Stem Cell Res Ther*. 2024;15(1):300. <https://doi.org/10.1186/s13287-024-03926-7>.
- Wang K, Jiang Z, Webster KA, Chen J, Hu H, Zhou Y, Zhao J, Wang L, Wang Y, Zhong Z, Ni C, Li Q, Xiang C, Zhang L, Wu R, Zhu W, Yu H, Hu X, Wang J. Enhanced cardioprotection by human endometrium mesenchymal stem cells driven by exosomal MicroRNA-21. *Stem Cells Transl Med*. 2017;6(1):209–22. <https://doi.org/10.5966/sctm.2015-0386>.
- Marinero F, Gomez-Serrano M, Jorge I, Silla-Castro JC, Vazquez J, Sanchez-Margallo FM, Blazquez R, Lopez E, Alvarez V, Casado JG. Unraveling the molecular signature of extracellular vesicles from endometrial-derived mesenchymal stem cells: potential modulatory effects and therapeutic applications. *Front Bioeng Biotechnol*. 2019;7:431. <https://doi.org/10.3389/fbioe.2019.00431>.
- Chen Q, Shao B, Xu YN, Li X, Ren SH, Wang HD, Zhang JY, Sun CL, Liu T, Xiao YY, Zhao PY, Yang GM, Liu X, Wang H. IGF2 contributes to the immunomodulatory effects of exosomes from endometrial regenerative cells on experimental colitis. *Int Immunopharmacol*. 2024;140:112825. <https://doi.org/10.1016/j.intimp.2024.112825>.
- Hida N, Nishiyama N, Miyoshi S, Kira S, Segawa K, Uyama T, Mori T, Miyado K, Ikegami Y, Cui C, Kiyono T, Kyo S, Shimizu T, Okano T, Sakamoto M, Ogawa S, Umezawa A. Novel cardiac precursor-like cells



- from human menstrual blood-derived mesenchymal cells. *Stem Cells*. 2008;26(7):1695–704. <https://doi.org/10.1634/stemcells.2007-0826>.
14. Dominici M, Le Blanc K, Mueller I, Slaper-Cortenbach I, Marini F, Krause D, Deans R, Keating A, Prockop D, Horwitz E. Minimal criteria for defining multipotent mesenchymal stromal cells. *Int Soc Cell Therapy Posit State Cytotherapy*. 2006;8(4):315–7. <https://doi.org/10.1080/14653240600855905>.
  15. Thery C, Amigorena S, Raposo G, Clayton A. Isolation and characterization of exosomes from cell culture supernatants and biological fluids. *Curr Protoc Cell Biol Chapter*. 2006. <https://doi.org/10.1002/0471143030.cb0322330>.
  16. Lan X, Hu YH, Li X, Kong DJ, Qin YF, Wang H. Oxymatrine protects cardiac allografts by regulating immunotolerant cells. *Int Immunopharmacol*. 2021;100:108080. <https://doi.org/10.1016/j.intimp.2021.108080>.
  17. Ramesh G, Ranganathan P. Mouse models and methods for studying human disease, acute kidney injury (AKI). *Methods Mol Biol*. 2014;1194:421–36. [https://doi.org/10.1007/978-1-4939-1215-5\\_24](https://doi.org/10.1007/978-1-4939-1215-5_24).
  18. Wang Y, Quan F, Cao Q, Lin Y, Yue C, Bi R, Cui X, Yang H, Yang Y, Birnbaumer L, Li X, Gao X. Quercetin alleviates acute kidney injury by inhibiting ferroptosis. *J Adv Res*. 2021;28:231–43. <https://doi.org/10.1016/j.jare.2020.07.007>.
  19. Ascon DB, Lopez-Briones S, Liu M, Ascon M, Savransky V, Colvin RB, Soloski MJ, Rabb H. Phenotypic and functional characterization of kidney-infiltrating lymphocytes in renal ischemia reperfusion injury. *J Immunol*. 2006;177(5):3380–7. <https://doi.org/10.4049/jimmunol.177.5.3380>.
  20. Gharraie S, Lee K, Newman-Rivera AM, Xu J, Patel SK, Gooya M, Arend LJ, Raj DS, Pluznick J, Parikh C, Noel S, Rabb H. Microbiome modulation after severe acute kidney injury accelerates functional recovery and decreases kidney fibrosis. *Kidney Int*. 2023;104(3):470–91. <https://doi.org/10.1016/j.kint.2023.03.024>.
  21. Ying W, Cheruku PS, Bazer FW, Safe SH, Zhou B. Investigation of macrophage polarization using bone marrow derived macrophages. *J Vis Exp*. 2013. <https://doi.org/10.3791/50323>.
  22. Noel S, Lee K, Gharraie S, Kurzhagen JT, Pierorazio PM, Arend LJ, Kuchroo VK, Cahan P, Rabb H. Immune checkpoint molecule TIGIT regulates kidney T cell functions and contributes to AKI. *J Am Soc Nephrol*. 2023;34(5):755–71. <https://doi.org/10.1681/ASN.0000000000000063>.
  23. Sheu KM, Hoffmann A. Functional hallmarks of healthy macrophage responses: their regulatory basis and disease relevance. *Annu Rev Immunol*. 2022;40:295–321. <https://doi.org/10.1146/annurev-immunol-101320-031555>.
  24. Liu K, Zhao E, Ilyas G, Lalazar G, Lin Y, Haseeb M, Tanaka KE, Czaja MJ. Impaired macrophage autophagy increases the immune response in obese mice by promoting proinflammatory macrophage polarization. *Autophagy*. 2015;11(2):271–84. <https://doi.org/10.1080/15548627.2015.1009787>.
  25. Chen XS, Wang SH, Liu CY, Gao YL, Meng XL, Wei W, Shou ST, Liu YC, Chai YF. Losartan attenuates sepsis-induced cardiomyopathy by regulating macrophage polarization via TLR4-mediated NF-kappaB and MAPK signaling. *Pharmacol Res*. 2022;185:106473. <https://doi.org/10.1016/j.phrs.2022.106473>.
  26. Ikeda M, Prachasilchai W, Burne-Taney MJ, Rabb H, Yokota-Ikeda N. Ischemic acute tubular necrosis models and drug discovery: a focus on cellular inflammation. *Drug Discov Today*. 2006;11(7–8):364–70. <https://doi.org/10.1016/j.drudis.2006.02.010>.
  27. Friedewald JJ, Rabb H. Inflammatory cells in ischemic acute renal failure. *Kidney Int*. 2004;66(2):486–91. [https://doi.org/10.1111/j.1523-1755.2004.761\\_3.x](https://doi.org/10.1111/j.1523-1755.2004.761_3.x).
  28. Swaminathan M, Kopyt N, Atta MG, Radhakrishnan J, Umanath K, Nguyen S, O'Rourke B, Allen A, Vaninov N, Tilles A, LaPointe E, Blair A, Gemmiti C, Miller B, Parekkadan B, Barcia RN. Pharmacological effects of ex vivo mesenchymal stem cell immunotherapy in patients with acute kidney injury and underlying systemic inflammation. *Stem Cells Transl Med*. 2021;10(12):1588–601. <https://doi.org/10.1002/sctm.21-0043>.
  29. Chen L, Qu J, Cheng T, Chen X, Xiang C. Menstrual blood-derived stem cells: toward therapeutic mechanisms, novel strategies, and future perspectives in the treatment of diseases. *Stem Cell Res Ther*. 2019;10(1):406. <https://doi.org/10.1186/s13287-019-1503-7>.
  30. Bozorgmehr M, Gurung S, Darzi S, Nikoo S, Kazemnejad S, Zarnani AH, Gargett CE. Endometrial and menstrual blood mesenchymal stem/stromal cells: biological properties and clinical application. *Front Cell Dev Biol*. 2020;8:497. <https://doi.org/10.3389/fcell.2020.00497>.
  31. Chen L, Xiang B, Wang X, Xiang C. Exosomes derived from human menstrual blood-derived stem cells alleviate fulminant hepatic failure. *Stem Cell Res Ther*. 2017;8(1):9. <https://doi.org/10.1186/s13287-016-0453-6>.
  32. Song A, Zhang S, Zhao X, Wu S, Qi X, Gao S, Qi J, Li P, Tan J. Exosomes derived from menstrual blood stromal cells ameliorated premature ovarian insufficiency and granulosa cell apoptosis by regulating SMAD3/AKT/MDM2/P53 pathway via delivery of thrombospondin-1. *Biomed Pharmacother*. 2023;166:115319. <https://doi.org/10.1016/j.biopha.2023.115319>.
  33. Xu Y, Ren S, Wang H, Qin Y, Liu T, Sun C, Xiao Y, Shao B, Zhang J, Chen Q, Zhao P, Yang G, Liu X, Wang H. Endometrial regeneration cell-derived exosomes loaded with siSLAMF6 inhibit cardiac allograft rejection through the suppression of desialylation modification. *Cell Mol Biol Lett*. 2024;29(1):128. <https://doi.org/10.1186/s11658-024-00645-y>.
  34. Ferrari D, Gambari R, Idzko M, Muller T, Albanesi C, Pastore S, La Manna G, Robson SC, Cronstein B. Purinergic signaling in scarring. *FASEB J*. 2016;30(1):3–12. <https://doi.org/10.1096/fj.15-274563>.
  35. Grenz A, Zhang H, Eckle T, Mittelbronn M, Wehrmann M, Kohle C, Kloor D, Thompson LF, Osswald H, Eltzschig HK. Protective role of ecto-5'-nucleotidase (CD73) in renal ischemia. *J Am Soc Nephrol*. 2007;18(3):833–45. <https://doi.org/10.1681/ASN.2006101141>.
  36. Winzer R, Nguyen DH, Schoppmeier F, Cortesi F, Gagliani N, Tolosa E. Purinergic enzymes on extracellular vesicles: immune modulation on the go. *Front Immunol*. 2024;15:1362996. <https://doi.org/10.3389/fimmu.2024.1362996>.
  37. Zhai X, Chen K, Yang H, Li B, Zhou T, Wang H, Zhou H, Chen S, Zhou X, Wei X, Bai Y, Li M. Extracellular vesicles derived from CD73 modified human umbilical cord mesenchymal stem cells ameliorate inflammation after spinal cord injury. *J Nanobiotechnol*. 2021;19(1):274. <https://doi.org/10.1186/s12951-021-01022-z>.
  38. Nakao Y, Fukuda T, Zhang Q, Sanui T, Shinjo T, Kou X, Chen C, Liu D, Watanabe Y, Hayashi C, Yamato H, Yotsumoto K, Tanaka U, Taketomi T, Uchiyama T, Le AD, Shi S, Nishimura F. Exosomes from TNF-alpha-treated human gingiva-derived MSCs enhance M2 macrophage polarization and inhibit periodontal bone loss. *Acta Biomater*. 2021;122:306–24. <https://doi.org/10.1016/j.actbio.2020.12.046>.
  39. Zhang S, Li J, Li C, Xie X, He J, Ling F, Li B, Wu H, Li Z, Zhen J, Liu G. CD73-positive pediatric urethral mesenchymal stem-like cell-derived small extracellular vesicles stimulate angiogenesis. *Regen Ther*. 2024;25:77–84. <https://doi.org/10.1016/j.reth.2023.12.002>.
  40. Duan Y, Chen X, Shao H, Li Y, Zhang Z, Li H, Zhao C, Xiao H, Wang J, Zhang X. Enhanced immunosuppressive capability of mesenchymal stem cell-derived small extracellular vesicles with high expression of CD73 in experimental autoimmune uveitis. *Stem Cell Res Ther*. 2024;15(1):149. <https://doi.org/10.1186/s13287-024-03764-7>.
  41. Umansky V, Shevchenko I, Bazhin AV, Utikal J. Extracellular adenosine metabolism in immune cells in melanoma. *Cancer Immunol Immunother*. 2014;63(10):1073–80. <https://doi.org/10.1007/s00262-014-1553-8>.
  42. Alcedo KP, Bowser JL, Snider NT. The elegant complexity of mammalian ecto-5'-nucleotidase (CD73). *Trends Cell Biol*. 2021;31(10):829–42. <https://doi.org/10.1016/j.tcb.2021.05.008>.
  43. Huen SC, Cantley LG. Macrophages in renal injury and repair. *Annu Rev Physiol*. 2017;79:449–69. <https://doi.org/10.1146/annurev-physiol-022516-034219>.
  44. Huen SC, Cantley LG. Macrophage-mediated injury and repair after ischemic kidney injury. *Pediatr Nephrol*. 2015;30(2):199–209. <https://doi.org/10.1007/s00467-013-2726-y>.
  45. Jang HR, Rabb H. Immune cells in experimental acute kidney injury. *Nat Rev Nephrol*. 2015;11(2):88–101. <https://doi.org/10.1038/nrneph.2014.180>.
  46. Maryam B, Smith ME, Miller SJ, Natarajan H, Zimmerman KA. Macrophage ontogeny, phenotype, and function in ischemia reperfusion-induced injury and repair. *Kidney*. 2024;5(3):459–70. <https://doi.org/10.34067/KID.0000000000000376>.
  47. Mao R, Wang C, Zhang F, Zhao M, Liu S, Liao G, Li L, Chen Y, Cheng J, Liu J, Lu Y. Peritoneal M2 macrophage transplantation as a potential cell therapy for enhancing renal repair in acute kidney injury. *J Cell Mol Med*. 2020;24(6):3314–27. <https://doi.org/10.1111/jcmm.15005>.

48. Vinuesa E, Hotter G, Jung M, Herrero-Fresneda I, Torras J, Sola A. Macrophage involvement in the kidney repair phase after ischaemia/reperfusion injury. *J Pathol*. 2008;214(1):104–13. <https://doi.org/10.1002/path.2259>.
49. Huang J, Cao H, Cui B, Ma X, Gao L, Yu C, Shen F, Yang X, Liu N, Qiu A, Cai G, Zhuang S. Mesenchymal stem cells-derived exosomes ameliorate ischemia/reperfusion induced acute kidney injury in a porcine model. *Front Cell Dev Biol*. 2022;10:899869. <https://doi.org/10.3389/fcell.2022.899869>.
50. Vallon V, Muhlbauer B, Osswald H. Adenosine and kidney function. *Physiol Rev*. 2006;86(3):901–40. <https://doi.org/10.1152/physrev.00031.2005>.
51. Hasko G, Pacher P. Regulation of macrophage function by adenosine. *Arterioscler Thromb Vasc Biol*. 2012;32(4):865–9. <https://doi.org/10.1161/ATVBAHA.111.226852>.
52. Garcia GE, Truong LD, Li P, Zhang P, Du J, Chen JF, Feng L. Adenosine A2A receptor activation and macrophage-mediated experimental glomerulonephritis. *FASEB J*. 2008;22(2):445–54. <https://doi.org/10.1096/fj.07-8430com>.
53. Hasko G, Pacher P, Deitch EA, Vizi ES. Shaping of monocyte and macrophage function by adenosine receptors. *Pharmacol Ther*. 2007;113(2):264–75. <https://doi.org/10.1016/j.pharmthera.2006.08.003>.
54. Yuan Q, Tang B, Zhang C. Signaling pathways of chronic kidney diseases, implications for therapeutics. *Signal Transduct Target Ther*. 2022;7(1):182. <https://doi.org/10.1038/s41392-022-01036-5>.
55. Orsini EM, Perelas A, Southern BD, Grove LM, Olman MA, Scheraga RG. Stretching the Function of Innate Immune Cells. *Front Immunol*. 2021;12:767319. <https://doi.org/10.3389/fimmu.2021.767319>.
56. Galgaro BC, Beckenkamp LR, van den Martha MN, Korb VG, Naasani LIS, Roszek K, Wink MR. The adenosinergic pathway in mesenchymal stem cell fate and functions. *Med Res Rev*. 2021;41(4):2316–49. <https://doi.org/10.1002/med.21796>.
57. Teo KYW, Zhang S, Loh JT, Lai RC, Hey HWD, Lam KP, Lim SK, Toh WS. Mesenchymal stromal cell exosomes mediate m2-like macrophage polarization through CD73/Ecto-5'-nucleotidase activity. *Pharmaceutics*. 2023. <https://doi.org/10.3390/pharmaceutics15051489>.
58. Sun Z, Kang J, Yang S, Zhang Y, Huang N, Zhang X, Du G, Jiang J, Ning B. CD73 inhibits titanium particle-associated aseptic loosening by alternating activation of macrophages. *Int Immunopharmacol*. 2023;122:110561. <https://doi.org/10.1016/j.intimp.2023.110561>.
59. Zhang S, Chuah SJ, Lai RC, Hui JHP, Lim SK, Toh WS. MSC exosomes mediate cartilage repair by enhancing proliferation, attenuating apoptosis and modulating immune reactivity. *Biomaterials*. 2018;156:16–27. <https://doi.org/10.1016/j.biomaterials.2017.11.028>.
60. Deng Y, Chen Q, Yang X, Sun Y, Zhang B, Wei W, Deng S, Meng J, Hu Y, Wang Y, Zhang Z, Wen L, Huang F, Wan C, Yang K. Tumor cell senescence-induced macrophage CD73 expression is a critical metabolic immune checkpoint in the aging tumor microenvironment. *Theranostics*. 2024;14(3):1224–40. <https://doi.org/10.7150/thno.91119>.
61. Zarrabi M, Shahrabaf MA, Nouri M, Shekari F, Hosseini SE, Hashemian SR, Aliannejad R, Jamaati H, Khavandgar N, Alemi H, Madani H, Nazari A, Amini A, Hassani SN, Abbasi F, Jarooghi N, Fallah N, Taghiyar L, Ganjibakhsh M, Hajizadeh-Saffar E, Vosough M, Baharvand H. Allogenic mesenchymal stromal cells and their extracellular vesicles in COVID-19 induced ARDS: a randomized controlled trial. *Stem Cell Res Ther*. 2023;14(1):169. <https://doi.org/10.1186/s13287-023-03402-8>.
62. Zamanian MH, Norooznezhad AH, Hosseinkhani Z, Hassaninia D, Mansouri F, Vaziri S, Payandeh M, Heydarpour F, Kiani S, Shirvani M, Rajati M, Bakhtiari M, Esmaili F, Yarani R, Mansouri K. Human placental mesenchymal stromal cell-derived small extracellular vesicles as a treatment for severe COVID-19: a double-blind randomized controlled clinical trial. *J Extracell Vesicles*. 2024;13(7):e12492. <https://doi.org/10.1002/jev2.12492>.
63. Bolandnazar NS, Raeissadat SA, Haghighatkah H, Rayegani SM, Oshnari RS, Keshel SH, Zahraei M, Aalipour K, Babaee M, Zamani A, Rad ZB, Soleimani M, Sefat F. Safety and efficacy of placental mesenchymal stromal cells-derived extracellular vesicles in knee osteoarthritis: a randomized, triple-blind, placebo-controlled clinical trial. *BMC Musculoskelet Disord*. 2024;25(1):856. <https://doi.org/10.1186/s12891-024-07979-w>.

## Publisher's Note

Springer Nature remains neutral with regard to jurisdictional claims in published maps and institutional affiliations.